

FEHM: A control volume finite element code for simulating subsurface multi-phase multi-fluid heat and mass transfer

May 18, 2007 LAUR-07-3359

George Zyvoloski
Technical Staff Member
Earth and Environmental Sciences Division
Los Alamos National Laboratory
Los Alamos, NM 87544

ABSTRACT

The Subsurface Flow and Transport Team at the Los Alamos National Laboratory (LANL) has been involved in large scale projects including performance assessment of Yucca Mountain, Environmental Remediation of the Nevada Test Site, the LANL Groundwater Protection Program and geologic CO₂ sequestration. Subsurface physics has ranged from single fluid/single phase fluid flow when simulating basin scale groundwater aquifers to multi-fluid/multi-phase fluid flow when simulating the movement of air and water (with boiling and condensing) in the unsaturated zone surrounding a potential nuclear waste storage facility. These and other projects have motivated the development of software to assist in both scientific discovery and technical evaluation. LANL's FEHM (Finite Element Heat and Mass) computer code simulates complex coupled subsurface processes as well flow in large and geologically complex basins. Its development has spanned several decades; a time over which the art and science of subsurface flow and transport simulation has dramatically evolved. For most early researchers, models were used primarily as tools for understanding subsurface processes. Subsequently, in addition to addressing purely scientific questions, models were used in technical evaluation roles. Advanced model analysis requires a detailed understanding of model errors (numerical dispersion and truncation) as well as those associated with the application (conceptual and calibration) Application errors are evaluated through exploration of model and parameter sensitivities and uncertainties. The development of FEHM has been motivated subsurface physics of applications and also by the requirements of model calibration, uncertainty quantification, and error analysis. FEHM possesses unique features and capabilities that are of general interest to the subsurface flow and transport community and it is well suited to hydrology, geothermal, and petroleum reservoir applications. As the creator and lead developer of FEHM, I will outline the development history of FEHM, describe its general software structure and numerical formulations, and some of its unique features. These features range from novel representations of equations of state to features that allow accurate representation of wellbores and other sub-grid scale phenomena. I will also compare the numerical method used in FEHM, the control volume finite element method (CVFE) with the finite element (FE) method, the finite difference (FD) method, and the integrated finite difference (IFD) method. Finally I compare FEHM with other software of which I am familiar.

OUTLINE

The **BACKGROUND AND HISTORICAL DEVELOPMENT** section traces the historical development of FEHM. This essentially mirrors the evolution of the control volume finite element method (CVFE) method and the simulation of coupled subsurface physics including, most notably, heat. The **NUMERICAL FORMULATION SUMMARY** outlines the CVFE method and compares it to finite element (FE), finite difference (FD) and integrated finite difference (IDF) methods. **SUBSURFACE PHYSICIS** section briefly describes the physics packages available and the associated variables. **SOLUTION OF THE NONLINEAR EQUATIONS** section describes how FEHM solves the nonlinear algebraic equations representing the coupled mass and energy balance equations. The Newton-Raphson method (with analytical derivatives), various pre-conditioning and degree-of-freedom reduction schemes, and the preconditioned Krylov space solver for linear equation, are explained. The **TOOLS FOR QUANTITATIVE ANALYSIS** section outlines the issues associated with quantifying errors when representing hydrostratigraphy on numerical grids, including a discussion of the impacts of grid generation. This section also lists external software and interfaces frequently used with FEHM during model calibration and uncertainty/sensitivity analyses. The section titled **EXPLOITING UNSTRUCTURED GRIDS** discusses several unique FEHM features that make use of the unstructured grid connectivity to couple models developed with different software. It includes an account of how FEHM efficiently generates and solves double porosity models and how wellbores can be “dropped into” pre-existing numerical grids. The section titled **APPLICATIONS** give a brief overview of current applications. The **FEHM CODE STRUCTURE AND INPUT** section outlines the basic workings of FEHM and describes features that facilitate model testing. Finally, the **RESEARCH PRIORITIES** section describes several active research areas being pursued in the development of FEHM and the **CONCLUSION** section draws some general conclusions.

This article does not describe the extensive transport capabilities of FEHM that includes multi-species advection/dispersion, coupled reactive geochemistry, and particle tracking (see Viswanathan, 1996, Viswanathan et al., 1998; Hammond, 1999, and Robinson et al., 2000 for details). The fully coupled, thermal-hydrologic and mechanical (THM) module is also not described other than noting the extra stiffness matrix terms required over those needed for the flow and transport solution and the suitability of the CVFE method for these applications. See Kelkar and Zyvoloski (1992) and Bower and Zyvoloski (1997) for details on this capability.

BACKGROUND AND HISTORICAL DEVELOPMENT

The numerical background of the FEHM computer code can be traced to the early 1970s. Before this time, finite element methods were almost exclusively used in solid mechanics, not flow problems. Applications to field problems (heat conduction) were being published, but nonlinear groundwater applications were rare; Neuman and

Witherspoon (1970), Neuman (1973), and Dalen (1979) were notable exceptions. Neuman (1973) solved the unsaturated-saturated zone flow equations with a free water table using a traditional finite element code. Table 1 summarizes the historical development of FEHM. Zyvoloski et al. (1976) published a finite element solution to unsaturated zone equations with application to shallow infiltration. The formulation Zyvoloski et al. (1976) used was different from previous finite element formulations in that the equations were developed by node rather than by element. They also expanded the nonlinear hydraulic conductivity in low-order, finite element basis functions instead of the usual method of evaluating these nonlinearities at integration (quadrature) points or as element averages. The element stiffness coefficients were then formed analytically. These procedures effectively separated the fluid and geometric parts of the approximating algebraic equations in a manner similar to what later became known as the CVFE method. The details of this formulation are given by Zyvoloski (1975). The nodal construction of the equations also facilitated storage of neighboring nodes in modified compressed sparse row format (CSR) (George and Liu, 1981; Zyvoloski, 1983) where only the nonzero neighbors of the solution matrices are stored and the starting positions of each row are identified at the beginning of the connectivity array. While Zyvoloski et al. (1976) described the predecessor of the CVFE discretization currently used in FEHM, the formulation for fully coupled subsurface heat and mass transfer equations was developed while the author was a post-doctoral fellow at the University of Auckland, New Zealand. Here, motivated by the need to solve the two-phase coupled subsurface heat and fluid flow equations for geothermal applications, Zyvoloski et al. (1979) formulated the heat and mass balance equations in primitive (mass conservative) form rather than with the usual linearized equations (Mercer and Pinder, 1973). The equations were solved fully implicitly rather than using the Implicit Pressure Explicit Saturation (IMPES) formulation that was common at the time in petroleum industry software (Thomas, 1979). Zyvoloski et al. (1979) also used a FD formulation to discretize the fully coupled mass and energy balance equations because finite-element-based solutions to multiphase flow problems lack numerical stability (Mercer and Faust 1975; Faust and Mercer, 1976). Zyvoloski et al. (1979) used Newton-Raphson (NR) iteration and introduced a method for solving the coupled system with an algebraic reduction in the effective degrees of freedom from two unknowns per node to one unknown per node to effectively “pre-condition” the linear system of equations, the solution of which provides the NR variable updates. The details are described in the section entitled **SOLUTION OF THE NONLINEAR EQUATIONS**. After the solution of this reduced algebraic system of equations, the pre-factored variable is recovered through back-substitution. This method of solving the fully coupled heat and mass balance equations in geothermal reservoirs was extended to water, water vapor, heat, and non-condensable CO₂ gas by Zyvoloski and O’Sullivan (1980). The three independent variables in this application were again solved with an algebraic reduction of variables. These techniques, which solve the coupled heat and mass transfer equations, were combined with the early CVFE discretization work to form an early version of the current FEHM computer code. This combination of techniques was first described by Zyvoloski (1983). Similar to Zyvoloski et al. (1976), the finite element equations developed by Zyvoloski (1983) were constructed with the row and geometric part of the finite element stiffness matrix separated from the fluid part and stored in modified CSR format. This required that the equation parameters to be defined on nodes

rather than on elements. It was noted in the paper that using node point quadrature (also known as Lobatto quadrature) instead of the usual Gauss quadrature points resulted a diagonal capacitance matrix and the usual five point FD stencil for two-dimensional problems when applied to numerical grids constructed of orthogonal quadrilateral elements. The paper also studied the relative performance of the node point quadrature (equivalent to CVFE) and the Gauss quadrature (equivalent to the FE). It was concluded that the node point quadrature (CVFE-like) option performed better than the Gauss quadrature (FEM) option for the nonlinear convection-dominated problems studied.

The next breakthrough came in the iterative solution of linear equations, often known as the “inner” iteration when used with a NR “outer” iteration. In the early 1980s, pre-conditioned conjugate-gradient methods and their non-symmetric variants began to appear in petroleum industry software literature for multi-phase subsurface fluid flow applications (Behie and Vinsome, 1982). These applications were for structured FD grids and were not available for FE or CVFE codes. Zyvoloski (1986) developed a variably pre-conditioned Krylov acceleration method using ORTHOMIN acceleration with a modified CSR format. The pre-conditioning part of the algorithm consists of incomplete lower-upper (ILU) factorization, which starts with the nodal connectivity and adds connections during each factorization step. This was the first time that a preconditioner, based on incomplete factorization, was reported for an unstructured grid application. Instead of completing the LU process, only one or two factorization steps are performed. Thus the label $ILU(n)$, where ILU stands for incomplete LU factorization, and n represents the number of factorization steps. With $n = 1$, only those operations are done that affect matrix positions of the original connectivity. With $n = 2$, additional nodal connections occur and for a typical FD application, the connectivity for the ILU preconditioner is about 50% greater than the nodal connectivity for the FD grid stencil. With the structured connectivity of FD methods, additional connections for the factorization steps can be determined rather easily for a given node. FE and CVFE methods use an unstructured connectivity and a symbolic factorization must be done to determine the positions of additional terms that occur during the factorization steps. Zyvoloski (1986) obtained an order of magnitude decrease in computer runtime in addition to significantly less computer memory usage with this linear solver when compared with the direct solvers previously used in FEHM. This has been the ‘core’ linear equation solver in FEHM ever since. Conversations with Manteuffel (1980) helped guide this programming effort. The ORTHOMIN acceleration was replaced with the more efficient GMRES and BCGSTAB (van der Vorst, 1992) acceleration methods and there have also been improvements in the symbolic factorization. Additional details are provided in the **SOLUTION OF THE NONLINEAR EQUATIONS** section.

FEHM is a large computer code comprising roughly 450 subroutines and approximately 200,000 lines of code with development and usage guided by funding trends of our research group at LANL and major collaborators. Several hundred no-cost FEHM licenses to individuals and institutions have been distributed world wide. This paper summarizes FEHM in sufficient detail to inform the reader of most of FEHM’s capabilities. With the advent of FORTRAN 90, FEHM common blocks were replaced

with use modules and dynamic memory allocation. Continued releases of new versions generally represent additional capabilities.

NUMERICAL FORMULATION SUMMARY

In the author's opinion CVFE evolved from researchers need to solve nonlinear problems with finite elements. Besides the author's work the reader is referred to Forsyth (1990) and Fung (1992) for more detail. A detailed numerical development of the CVFE method used in FEHM is provided by Zyvoloski (2007). In the rest of this section a numerical definition of the CVFE method will be provided and the method will be compared to the finite element method (FEM), the finite difference method (FDM), and the integrated finite difference method (IFDM). Later in the paper, FEHM will be compared with several well known software packages.

As noted in the background section above, the finite element method can be made equivalent to the finite difference method by choosing quadrature points for the evaluation of the stiffness matrix integral that are positioned at the nodes. The nodal quadrature points make the inputting of parameters at nodes, like FD methods, very convenient. If these procedures are applied to orthogonal four node quadrilateral and hexahedral elements, the standard five point (2D) and seven point (3D) FD stencils result. If these procedures are applied to triangular or tetrahedral elements the result is a method equivalent to the IFD method (described later). The geometric terms associated with the CVFE method are defined in Figure 1. The internodal area divided by distance ($A_{ij}/\Delta d_{ij}$) term, also called the area factor, is defined for both orthogonal (Fig. 1a) and non orthogonal grids (Fig. 1b). The area factors are formed by the intersection of perpendicular bisectors (PEBI) of the edges of the elements. This ensures that the area factors are perpendicular to the control volume boundary. In particular, note the area factor A_{35} for the connection between nodes 3 and 5 is zero for the orthogonal grid and non zero for the non orthogonal grid. The resulting connectivity for the orthogonal case is the standard five-point FD stencil. The CVFE, block centered FD, and IFD methods would be equivalent on such (orthogonal) grids. In fact, the grid generation software typically used for large-scale FEHM applications, the Los Alamos Grid Toolkit (LaGriT, 2007) generates nodal volumes and area factors ($A_{ij}/\Delta d_{ij}$) from a finite element definition of triangles (with unit depth), tetrahedrals, quadrilaterals (with unit depth), and hexahedrals. In this author's opinion the only difference between IFD and CVFE methods is the underlying finite element grid which accompanies the CVFE method.

Comparison with the FE method. CVFE methods have several advantages compared to the traditional FE method when used to simulate unsaturated groundwater flow. Consider the equation for the conservation of water in the unsaturated zone:

$$\frac{\partial(\theta\rho_w\phi)}{\partial t} = \nabla \cdot \left[\frac{k\rho_w}{\mu_w} k'(\theta)(\nabla p_w - \rho_w g z) \right] \quad (1)$$

where θ is saturation, ρ_w is the water density, ϕ is the porosity, t is the time, z is elevation, g is the gravitational constant, μ_w is viscosity, p_w is pressure, k is intrinsic permeability and $k'(\theta)$ is relative permeability. Equation 1 can be highly nonlinear and is equivalent to Richards' Equation (Richards, 1931) with the specification of a capillary relationship between θ and p_w . For unconditional stability, the nonlinear relative permeability, $k'(\theta)$, must be upwinded in any numerical method. For FE methods, this is either not done or it is computationally inefficient because of the necessity to recompute the stiffness matrix. For the CVFE method, it is easy. Because of the nodal input of parameters, the separation of the geometric and the nodal nonlinear terms, and the node by node assembly of the numerical analog of Eq. 1, the CVFE method naturally identifies node pairs and can apply any internodal evaluation technique, including harmonic averaging or upwinding, at the control volume boundary. While FEHM users have the ability to choose the internodal evaluation method, they are always recommended to use full upwinding for nonlinear or advective terms. The nodal connectivity is contained in compressed sparse row (CSR) format as opposed to the element connectivity array that is typical of FE methods. The nodal connectivity greatly facilitates the formulation of nonlinear equations (requiring upwinding) in a Newton Raphson (NR) iteration rather than the Picard iteration commonly found in FE software. This in turn results in the CVFE method having greater computational efficiency than FE method.

It should be noted here that all control volume discretization methods (FD, IFD, CVFE) have an advantage over typical FE methods in mass conservation. These methods are locally conservative and the standard FE method is not. Mixed FE methods do conserve mass locally, but at a considerable cost in efficiency. The lack of local mass conservation has the potential to cause significant errors in nonlinear problems with large grid changes.

This author sees no disadvantages in the CVFE method compared to the FE method for highly nonlinear subsurface flow applications (e. g. Richards' Equation). For the solution of large scale confined aquifer applications, a linear problem requiring no iteration, there might be little difference between the two methods.

Comparison with the FD method. It was noted previously that the CVFE method applied on a grid with orthogonal quadrilaterals (2D) or hexahedrals (3D) produced the standard five point and seven point finite difference stencils. The two methods both readily implement upwinding and NR iteration in the solution of nonlinear equations. The CFVE method has significant advantage in that it can also build control volumes from triangles and tetrahedrals. This allows spatially variable hydrostratigraphy and other internal boundaries to be represented accurately. Figures 2 and 3 give examples of CVFE grids with grid resolution that varies in accordance with stratigraphic constraints. Additional discussion will occur when **quality** grids are presented.

Traditional FD methods embodied in the popular MODFLOW (Harbaugh et al., 2000) software package have a structured connectivity that allows the neighboring nodes to be identified without the use of either an element or nodal connectivity array. Efficient software is readily available for structured connectivity that solves the linear equations that result from the finite difference equations. This gives a computational advantage in both speed and computer memory requirements over the FE, IFD, and CVFE methods that use unstructured connectivity. Zyvoloski and Vessilinov (2006) estimated that the penalty for unstructured connectivity was 20 -50 % extra CPU time to solve an identical problem. Because the FE method must recalculate the stiffness matrix at each iteration, this penalty is greater, for problems requiring iteration, for the FE method than the CVFE method which separates the nonlinear and geometric parts on the internodal flux terms. There is considerable extra storage required for the unstructured connectivity methods. This will be discussed later when FEHM is compared to the FD code MODFLOW. These disadvantages disappear when a fine resolution region is required in a large numerical grid. Here, the fine resolution will propagate to the boundary in the FD method, often referred to as streaking, whereas the unstructured methods have the ability to localize the refinement. Localization can only be achieved with a FD method through iteration, with additional model runs, of the solutions on the fine grid and coarse grid parts of the problem (Mehl and Hill, 2002).

Comparison with the IFD method. In many applications the IFD and CVFE methods are identical. One of the most well known IFD based computer codes, TOUGH2 (Pruess, 1991), needs a connectivity matrix, nodal coordinates, nodal volumes, and control volume face areas to be provided to the code as input data. For relatively complicated problems, this is accomplished by external grid generation software. Internally, FD, IFD and CVFE solve the same numerical equations. For Eq. 1 this would be:

$$V_i \frac{[(\rho_w \phi)_i^{n+1} - (\rho_w \phi)_i^n]}{\Delta t} - \sum_{\text{neighbor cells}} \left(\frac{k'(\theta) k \rho_w}{\mu_w} \right)_{ij} \cdot \left(\frac{A_j}{\Delta d_{ij}} \right) \cdot [(p_{wj} - p_{wi}) - (\rho_w g)_{ij} (z_j - z_i)] = 0 \quad (2)$$

The summation refers to neighboring nodes, j , connected to node i . Here the $()_{ij}$ represents some inter-nodal averaging. The term V_i is the volume of the gridblock surrounding node i . The area factor $(A_{ij}/\Delta d_{ij})$ has been described earlier. Harmonic, arithmetic, and upwinded internodal evaluation can all be used with the IFD method. The upwinding of the two point fluxes (depending only on i and j nodes) facilitates stable and monotonic numerical simulation of multiphase flow.

Differences between the IFD and CVFE methods are largely based on where and when the gridblock volume and area factors are calculated. IFD methods do not have an underlying FE grid. In CVFE software (e. g. FEHM or LaGRit) the traditional FE element definitions and nodal coordinates are inputs and they are used to calculate both the nodal connectivity and the area factors. If the elements used are orthogonal (or right triangles and right tetrahedrals) both methods will produce identical connectivities and area factors. This is shown in Figure 1a. Note that the areas are constructed by the PEBI

method described earlier and this leads naturally to zero diagonal area (i.e., $A_{35} = 0$) in Figure 1a and the elimination of the diagonal connection. This results in the standard FD stencil. If the elements are non orthogonal as is shown in Figure 1b, then the CVFE software will *automatically* add connections during the course of creating the area factors as required to produce a **quality** grid (discussed later). The IFD software requires that nodal connectivities (not element definitions) be provided as input. Thus, the additional connections required for non orthogonal grids are not easy to obtain. As a practical approach, IFD methods often ignore the requirement of additional terms and use a simple FD stencil (Haukwa et al., 2003) even on non orthogonal grids. The CVFE method naturally conserves computer memory by only adding additional connections where required by grid geometry.

The second difference is that the stiffness matrix calculations available with the CVFE method as part of its FE legacy are invaluable when coupling the thermal, hydrologic, and mechanical behavior (THM). In a CVFE code, the variables and equation parameters for both the flow and stress equations are co-located at gridblock centers and the non isotropic terms (e. g. the xy, xz, yz terms) needed for the stress equations are easily calculated. This functionality is not available in IFD software; the fully coupled THM simulations are difficult if not impossible in IFD software. This functionality is available in FE software and coupling would be possible for mildly nonlinear problems with the caveats listed previously in the discussion on the comparison between the FE and CVFE methods.

SUBSURFACE PHYSICIS

FEHM contains a large suite of subsurface physics modules that are used for a variety of applications. Table 2 lists the physics modules that are tested and in common use. The table also includes the primary variable set and selected references. The oldest module is the water, water vapor, and energy flow that has been used for geothermal applications. Of particular interest to geothermal applications is the inclusion (in the usual suite of rock compressibility of a nonlinear fracture opening relationship, the “Gangi model” (Gangi, 1978) that relates the permeability and aperture of fractures to fracture roughness and earth stresses. This relationship made it possible to accurately model a very complicated geothermal reservoir that was created through hydraulic fracturing (Tenma et. al., 2007). The newest physics module is the non isothermal CO₂-water module that is used in CO₂ sequestration studies. The module includes a novel tabular equation of state (EOS) that allows for efficient calculation of CO₂ properties and phase transitions even in the super critical range. This EOS formulation will be detailed shortly. In addition, feedback from the transport module (Robinson et. al, 2000) in FEHM is available in a timestep-lagged manner to the flow solution. For example, if the reactive transport solution in FEHM predicts that silica will precipitate in a fracture, then the porosity and permeability can be changed accordingly. Of course, any explicit update will put limitations on the time step size.

While FEHM uses several different functional representations for the EOS of fluids and rock parameters, two that are unique to FEHM are worth mentioning. The first is the use

of rational polynomials is the EOS for water and water vapor. Rational function approximations and innovative tabular equations of state facilitate the evaluation analytical derivatives in FEHM's NR iteration. Rational function approximations (ratios of polynomials) accurately represent water properties (less than a few tenths of percent error over the ranges given above) while providing derivatives, because of the polynomial functions, at virtually no additional CPU cost. Complete third-order polynomials in pressure and temperature are used in both the numerator and denominator. For example, the density is approximated as:

$$\rho(P,T) = \frac{Y(P,T)}{Z(P,T)}, \quad (3)$$

where

$$Y(P,T) = Y_0 + Y_1P + Y_2P^2 + Y_3P^3 + Y_4T + Y_5T^2 + Y_6T^3 + Y_7PT + Y_8P^2T + Y_9PT^2, \quad (4)$$

and

$$Z(P,T) = Z_0 + Z_1P + Z_2P^2 + Z_3P^3 + Z_4T + Z_5T^2 + Z_6T^3 + Z_7PT + Z_8P^2T + Z_9PT^2. \quad (5)$$

This type of relationship provides an accurate method for determining parameter values over a wide range of pressures and temperatures, as well as allowing derivatives with respect to pressure and temperature to be computed easily (Zyvoloski et al., 1992). Polynomial coefficients were obtained using a Levenberg-Marquardt-based minimization method with a differential correction algorithm (Blackett, 1996) to fit data from the National Bureau of Standards OSRD Database 10, the database used for the NBS/NRC Steam Tables (Harr et al., 1984). The properties of the liquid (water) and water vapor phases are represented over wide range of pressures (0.001 to 110 MPa) and temperatures (0.5 to 360°C).

The other unique EOS uses a variably-spaced tabular lookup tables for representing the properties of CO₂ in all phase states including "supercritical fluid". The details are described in Doherty (2006). The method may be outlined with the aid of Figure 4 and Figure 5. Figure 4 depicts how a phase transition line (ie. the saturation line) is represented in a variably-spaced grid. This arrangement allows very fine grid spacing in areas where properties change rapidly, while not using massive amount of computer memory. In the tables of CO₂ properties in FEHM, temperature increments as low as 0.01°C are used near the critical point (7.38 Mpa, 31.1°C) and up to 1°C elsewhere. This allows the use of tables that have thousands to millions of points rather than billions of points. The data for both liquid and vapor and also stored in a single table in an intuitive and natural way. Figure 5 shows a close-up of an element of the lookup table that has a phase transition line. There is a property discontinuity at the liquid vapor interface and triangular interpolation is used on each side of the phase transition line. In a cell without the phase transition line, bilinear interpolation is used. With two phase calculations, the

temperature becomes a function of pressure and the above method smoothly represents this behavior because the phase transition line is an integral part of the table.

SOLUTION OF THE NONLINEAR EQUATIONS

The efficient solution of coupled nonlinear problems is critical to the simulation of large scale applications. FEHM uses a Newton-Raphson (NR) iteration (the “outer loop”) to solve the nonlinear material and energy balance equations. FEHM differs from similiar multi-physics computer codes (e.g. TOUGH2, see Pruess (1991), and NUFT, see Nitao(1998)) in that the NR derivatives are formed analytically, as opposed to numerically, because this generally leads to faster convergence of the very stiff nonlinear system of equations that often arise when investigating widely varying parameter sets as might be encountered during model calibration . However, it also can lead to slower development of new physics modules (i.e., tracking down programming errors). A porous flow simulator that solves energy and mass balance equations requires the functional dependence of the phase densities, the phase enthalpies, and the phase viscosities on T and P for all fluids in a system. For the NR iteration, FEHM requires the analytic derivatives of these thermodynamic functions with respect to P and T .

In the solution of the coupled heat and mass transfer equations, FEHM forms and evaluates all balance equations even though disparate spatial and temporal scale may render some of the balance equations relatively unimportant over some time periods. Consider the simultaneous solution of heat and mass transfer:

$$\begin{aligned}
 R_{mi} = V_i & \left[\frac{(\phi(\rho_l S_l + \rho_v S_v))_i^{n+1} - (\phi(\rho_l S_l + \rho_v S_v))_i^n}{\Delta t} \right. \\
 & - \sum_{\text{neighbor cells}} \left(\frac{k \rho_l}{\mu_l} R_l \right)_{ij} \cdot \left(\frac{A_{ij}}{\Delta d_{ij}} \right) \cdot \left[(P_{lj} - P_{li}) - (\rho_l g)_{ij} (z_j - z_i) \right] \\
 & \left. - \sum_{\text{neighbor cells}} \left(\frac{k \rho_v}{\mu_v} R_v \right)_{ij} \cdot \left(\frac{A_{ij}}{\Delta d_{ij}} \right) \cdot \left[(P_{vj} - P_{vi}) - (\rho_v g)_{ij} (z_j - z_i) \right] + q_{mi} \right] \quad (6)
 \end{aligned}$$

$$\begin{aligned}
R_{ei} = V_i & \frac{\left[((1-\phi)\rho_r u_r + \phi(\rho_l u_l S_l + \rho_v u_v S_v))_i^{n+1} - ((1-\phi)\rho_r u_r + \phi(\rho_l u_l S_l + \rho_v u_v S_v))_i^n \right]}{\Delta t} \\
& - \sum_{\text{neighbor cells}} \left(\frac{k \rho_l h_l}{\mu_l} R_l \right)_{ij} \cdot \left(\frac{A_{ij}}{\Delta d_{ij}} \right) \cdot \left[(P_{lj} - P_{li}) - (\rho_l g)_{ij} (z_j - z_i) \right] \\
& - \sum_{\text{neighbor cells}} \left(\frac{k \rho_v h_v}{\mu_v} R_v \right)_{ij} \cdot \left(\frac{A_{ij}}{\Delta d_{ij}} \right) \cdot \left[(P_{vj} - P_{vi}) - (\rho_v g)_{ij} (z_j - z_i) \right] \\
& - \sum_{\text{neighbor cells}} K_{ij} \cdot \left(\frac{A_{ij}}{\Delta d_{ij}} \right) \cdot (T_j - T_i) + q_{ei}
\end{aligned} \tag{7}$$

where, in addition to the parameters previously defined for equation for Eq. (1) and Eq. (2), u is the internal energy, h is the enthalpy, K is the thermal conductivity, and T is the temperature. The subscripts l and v refer, respectively, to the liquid and vapor phases and the subscripts m and e refers to the mass and energy balance equations respectively. The flow terms are evaluated at the current time step. The solution of the simultaneous set of equations (6) and (7) for the NR updates takes the form:

$$[A_{11}]\{x_1\} + [A_{12}]\{x_2\} = -\{R_m\}, \tag{8}$$

$$[A_{21}]\{x_1\} + [A_{22}]\{x_2\} = -\{R_e\}, \tag{9}$$

where $[A_{11}]$ and $[A_{12}]$ contains the derivatives with respect to x_1 and x_2 , respectively, for the mass balance equation. Here, x_1 is the pressure and x_2 is the energy variable, either temperature or saturation, depending on the phase state. All of the balance equations depend on both x_1 and x_2 and the matrices in equations (8) and (9) have off-diagonal terms that represent derivatives of the internodal flow terms with respect to the variables. We note, however, that the pressure (x_1) occurs explicitly in flow terms while energy variable (x_2) occurs implicitly in the internodal flow terms through the dependence of density, viscosity, and enthalpy on temperature and explicitly through the heat conduction term. The situation is the same if the energy variable “switches” to saturation in the two phase region. Because the time scale for a pressure pulse to travel is faster in general than that for a temperature or saturation wave, it is tempting to solve equation (6) and (7) sequentially. The solution is accomplished this way in several commercial FEM simulation packages. In FEHM, the solution is obtained using a fully coupled ILU(n)-Krylov space solver to solve the coupled equations (8) and (9) or with the reduced degree of freedom algorithm (RDOF) originally developed by Zyvoloski et al (1979) and subsequently improved. The algorithm neglects the off-diagonal contribution in A_{12} and A_{22} and thus allows a reduced one-degree-of-freedom algorithm to be formed:

$$\left[[A_{11}] - [A_{12}][A_{22}]^{-1}[A_{21}] \right] \{x_1\} = -\left\{ \{R_m\} - [A_{12}][A_{22}]^{-1}\{R_e\} \right\}. \tag{10}$$

The inverse operations in equation (10) is with a diagonal matrix. The NR correction for temperature (or saturation) can then be obtained through back substitution. The algorithm has similarities to the well-known IMPES algorithm (Watts, 1986) developed for the petroleum industry. Unlike schemes that employ the explicit solution of some parts of the balance equations, the RDOF methods are fully implicit and have no timestep limitation. If temperature effects start to dominate in equations (8) and (9), the RDOF method simply uses more iterations with the attendant timestep restarts when the iterations exceeded some predetermined limit. Zyvoloski (1989) showed that method could be improved by adding a number of successive over relaxation (SOR) steps of equations (8) and (9) after equation (10) was solved. Bullivant and Zyvoloski (1990) showed that the block normalization of equations (8) and (9) was equivalent to the matrix operations in equation (10). Tseng and Zyvoloski (2000) showed that RDOF operations could be done as part of the ILU pre-conditioner while using equations (8) and (9) for the GMRES acceleration. This was more robust in terms in that the RDOF method was no longer an approximate NR technique but became an efficient pre-conditioner. Tseng and Zyvoloski showed RDOF operations effectively solved multi-component heat and mass transfer equations and speedups of 30% or more are realized with the modern Krylov-space solvers. Moreover, this was accompanied with guaranteed savings of up to factor of ten (for three independent variables) in memory requirements.

Numerical ill-conditioning arising from disparate time scales of the different mass and energy balance equations, as well as differing control volume sizes, are attenuated in FEHM through block normalization of the balance equations and using a stopping criteria based on the residuals of the normalized equations. As mentioned previously, the just-described reduction algorithms always track the complete heat and mass transfer balance equations. This ensures that all linear equations are solved equitably; the nonlinear equations are considered solved when the maximum residual of block-normalized equations is smaller than a user-specified tolerance.

TOOLS FOR QUANTITATIVE ANALYSIS

The design and development of FEHM has mirrored the groundwater community's need for quantitative groundwater models. By quantitative analysis, it is meant that the model results, for example flow rates, are quantified in terms of parameter uncertainty, grid effects, etc. Zyvoloski and Vesselinov (2006) showed that improper grid resolution changed the values of calibrated permeability by up to an order of magnitude. The Yucca Mountain and environmental restoration programs at the Nevada Test Site require that the model errors and uncertainty be evaluated. While some errors, such as those associated with the conceptual model, will always be difficult to assess, others, such as those associated with grid block size and numerical difference method (truncation error), and the representation of hydrostratigraphy, are relatively straightforward to evaluate. Analyzing these errors in combination with model calibration, uncertainty analysis, and the evaluation of multiple conceptual models provides a quantitative framework for decision making. It must also be noted that the grid resolution and numerical

discretization method can greatly affect our ability to represent alternate conceptual models that involve faults or other features requiring fine grid resolution. The sub section **Quality grids** is unique in the sense that the CVFE method in FEHM and the LaGriT software allow, perhaps for the first time, the combined evaluation of both structural error (i.e the representation of hydrostratigraphy) and truncation error (grid size).

Quality grids. In a majority of large scale applications using FEHM, the numerical grid is based on a solid earth model of the hydrostratigraphy such as EarthVision (2007), Stratamodel (2007), or GoCad (2007). The generation of quality grids, those that satisfy the Voronoi criteria (Voronoi, 1908), is crucial to quantitative analysis of subsurface flow and transport. Gable et al. (1996) discusses many of the issues related to grid generation. Figure 2 and Figure 3 show two examples of grids created with LaGriT. Figure 2 illustrates the EarthVision solid model and numerical grid for the confined aquifer system at the Nevada Test Site (Ruskauff et al., 2006) based on control volumes generated from orthogonal hexahedral elements with octree refinement near faults and other geological features. The orthogonal elements facilitate the use of a velocity-based interpolation particle tracking method (Pollock, 1989) and the octree regions employ control volumes generated from tetrahedral elements. Figure 3 shows a tetrahedral-based grid, generated by LaGriT, of an unsaturated flow system near Los Alamos (Robinson et al, 2005). The linear features identified with increased resolution are fine-gridded, Voronoi-correct, faults have many extra connections compared to FD methods to ensure positive area factors. Evident in both figures are distinct, sloping hydrostratigraphic layers; the ability to represent these sloping layers can be important for complex flow geometries. Negative area factors can occur for some large angles between nodes or grid blocks. Most often, negative area factors can be corrected by increasing the grid resolution these areas when additional connectivity is easily incorporated (as is the case with the CVFE method). Figure 6 depicts an idealized sloping hydrostratigraphy that has been mapped on a grid with relatively coarse resolution. The mapping with an orthogonal FD grid not only looks blocky, but when used in simulations, it can lead to predictions that are orders of magnitude in error when compared to a fine-grid simulation for models with large (realistic) permeability contrasts between the layering (Zyvoloski and Vessilinov, 2006). The source of this error consists of both the mapping error associated with the hydrostratigraphy and the numerical truncation error associated with the numerical difference method. One way to estimate the combined hydrostratigraphic mapping and truncation errors is to map the hydrostratigraphic model onto a sequence of coarse to fine resolution grids and monitor the convergence of steady-state flow rates with simple fixed head boundary conditions. Bower et al. (2005) found this exercise useful as a means to determine an adequate grid resolution in each direction for flow and contaminant transport. Figure 7 shows the grids they used on the left while a plot of the total groundwater flow through the model as a function of the number of nodes in the model subject to head boundary conditions applied (separately) in the coordinate directions is on the right. Clearly, the north-south flow stabilizes quickly at low grid resolution while the other flow directions require much finer grid resolution. It is evident that the direction of flow in a given simulation is important in designing the appropriate grid resolution. Their work used orthogonal hexahedral elements that produced a standard seven point FD stencil for their three-dimensional simulations. CVFE variable connectivity is ideally

suites for grid generation tools that effectively represent the hydrostratigraphy with sloping grids. MODFLOW also allows the representation of sloping hydrostratigraphy while retaining the standard FD stencil. Figure 8 compares the standard five point FD stencil and associated control volume with the CVFE method when used with a sloping grid. Figure 8a shows the standard 5 point stencil when the gridblocks conform to the slope. The inconsistency in the control volume is evident. The CVFE method, adhering to Voronoi constraints, automatically adds additional connections and generates the grid stencil shown in Figure 8b. Here, two more connections are added to render the grid connections and areas consistent with the control volume. These extra connections are defined by precisely the process depicted in Figure 1. The inconsistent grid stencil shown in Figure 8a, labeled a conforming finite difference (CFD) stencil by Zyvoloski and Vessilinov (2006), has a component of the numerical truncation error that is proportional to the slope angle as well as the more common terms that depend on grid size. Although the grid-size terms decrease with grid size; the slope angle error remains constant. The argument has been made that the grid stencil shown in Figure 8a is adequate for sloping grids of less than ten degrees (Haukwa et al., 2003). Zyvoloski and Vessilinov, (2006) confirmed this for the coarse grid shown in Figure 8 and single phase flow. Here the errors in mapping of the hydrostratigraphy outweighed the truncation error. The problems with CFD stencils of the type shown in Figure 8 can be summarized as follows:

1. In a complex flow simulations with vertical and horizontal components, the relative magnitude of the flow components may differ by orders of magnitude yet the smaller component may be responsible for important phenomena like perching and contaminant transport. The question naturally arises: Does the error due to the slope angle in the CFD grid stencil overwhelm the true flow?
2. The CFD grid stencil creates uncertainties with grid testing convergence studies because the truncation error does not diminish to zero,
3. The errors associated with the CFD grid stencil creates uncertainties in calibrated models when used for predicting future behavior. This exacerbates the already dubious (but common) practice of using flow models for predicting transport. Here, gross regional flow may be adequately represented with the CFD method, while the contaminant transport, often originating from sources separated from the regional flow by confining layers, may be dominated by much finer flow field detail.

The errors incurred with CFD stencils when they are used with transport have also been reported by in Jenny et al., 2001). They performed grid tests using the five point FD stencil on non rectangular grids (i.e. the CFD stencil) and obtained the results shown in Figure 9. The results for the CFD are considerably different than the correct (flat interface) solution obtained with the 27 point stencil (equivalent to the CVFE stencil with distorted grids in 3D). The concerns raised in Jenny et al. (2001) transfer directly to any problem that uses upwinded transported parameters: advective transport, unsaturated zone flow, combined unsaturated zone and saturated zone flow, and buoyancy driven heat and mass transfer.

It should be noted also that FEHM also provides an internal FD grid generator to quickly scope problems and facilitate comparison to FD of CFD software.

Model calibration and uncertainty analysis. FEHM has made extensive use of external calibration software in many large-scale simulations. PEST (2007) uses an enhanced Levenberg-Marquardt algorithm and has a number of attractive features that facilitate uncertainty and sensitivity analyses (Moore and Doherty, 2005). Model calibration and uncertainty analysis for a large model with perhaps hundreds of calibration parameters often takes thousands of model runs. Codes using unstructured connectivity (FE, IDF, and CVFE methods) have many more startup operations than structured FD codes like MODFLOW. As mentioned earlier, FEHM facilitates multiple runs by reading in area factors and symbolic factorization connectivity in binary format. FEHM also has the option of being run as a subroutine from a driver program. This feature allows all of the startup calculations to be retained in memory and eliminates the need for input data (e.g., the permeability field) to be repeatedly loaded. Because of FEHM's long association with the PEST and its suite of utilities, it has a module (*pest*) that simplifies communication with the PEST software. FEHM is also being used with the global optimization software AMALGAM (Vrugt and Robinson, 2007). This software is particularly useful in those applications where the parameter sensitivities are discontinuous or there are many local minima (Vrugt, 2007). For large scale applications, model runs can number in the tens of thousands for calibration and uncertainty analyses and they are routinely distributed to multiple processors using utilities available with PEST as well as several developed at LANL.

EXPLOITING UNSTRUCTURED GRIDS

FEHM has exploited the unstructured grid connectivity in model coupling and localized grid resolution, the generalized dual-porosity method, and the embedded wellbore model. To the author's knowledge, the features are unique to FEHM.

Model Coupling. Model coupling (communication of different models through input and output files) was motivated by a desire to simulate entire groundwater basins. Basin-scale groundwater flow regions include surface, vadose zone, and deeper regional aquifers. Distinct regions can have different temporal and spatial characteristics (including grid resolution requirements) not to mention different numbers of independent variables per gridblock. To avoid problems associated with high-aspect-ratio finite difference cells (i.e. streaking), Mehl and Hill (2002) developed a local grid refinement method that couples a high resolution "child" grid to a coarse "parent" grid using an iterative technique that alternately mapped hydraulic head and flux fluxes onto parent and child interfaces. Chen and Zyvoloski (2006) were able to reproduce such local grid refinement without iteration using FEHM, a spatially variable grid, and octree refinement similar to that shown in Figure 2. Moreover, a saturated-unsaturated flow system solution with model coupling was feasible through either model iteration or a combined octree-refined model without iteration. To facilitate model coupling in FEHM a specific subroutine (*submodel_bc.f*) and input macro (*subm*) was created. The CVFE formulation makes the matching on gridblocks centers with a FD control volume code like

MODFLOW. Dickenson et al. (2007) developed a technique to couple FEHM and MODFLOW (Harbaugh et al., 2000) even when coupled grid (nodes or cell centers) were not coincident. In the future, model coupling, especially across different software and codes, may be an important aspect of large-scale computing because of the time and expense of data collection, conceptual model development, numerical model creation, and model calibration. One can easily imagine an existing basin-scale MODFLOW model coupled to FEHM in important areas surrounding contaminant sources. While MODFLOW typically has one independent variable, FEHM models may have several variables representing complex non isothermal vadose zone processes. Also, it should be noted that iterative model coupling is a necessary component in many parallelization schemes when models reside on different processors in a distributed computing environment. The Local Grid Refinement (LGR) package in MODFLOW (MODFLOW-LGR, 2005) also describes more details on model coupling.

Generalized Dual Porosity Method. While there has been considerable research in multiple porosity methods (Gerke and van Genuchten, 1993; Zyvoloski et al., 1992; Pruess and Narasimhan, 1985; and Warren and Root, 1963), none has exploited the computational advantages of unstructured grids and CSR storage. FEHM has a variety of different sub-grid scale features that include traditional dual permeability and dual porosity methods. They are summarized with references in Table 3. The basic idea of dual porosity methods is to represent subgrid-scale phenomena such as fractures or unconnected pore space as a part of a gridblock (Zyvoloski et al., 2007). The gridblock is divided as shown in Figure 10a with one primary node (mobile region) and one secondary node (immobile region). The dual porosity method assumes that the primary porosity connects globally to other primary nodes but the secondary node connects only to the primary node in its gridblock (the related dual permeability method allows both the primary and the secondary nodes to communicate globally). Because the dual porosity assumption is equivalent to a one-dimensional connection between the primary and secondary nodes, it allows the secondary nodes to be pre-factored with tridiagonal decomposition using the Thomas algorithm. This conceptualization of the secondary material communicating one dimensionally with the primary node does not limit the model to only a single secondary porosity, multiporosity modeling is allowable (Pruess and Narasimhan, 1985; Zyvoloski et al., 1992; Smith and Seth, 1999). Additional secondary nodes as shown in Figure 10b help represent steep gradients such as might occur with contaminants diffusing from a clay layer (immobile region) into a sandy aquifer (mobile). By using the flexibility inherent in the unstructured connectivity of FEHM, Zyvoloski et al. (2007) advanced the technology with the Generalized Dual Porosity Method (GDPM) where the number of secondary nodes connected to a primary node can vary spatially while maintaining the computationally efficient one-dimensional decomposition. For instance, in a heterogeneous flow system composed of clay and sand, double porosity nodes might be restricted to clay layers. To simplify the logic enabling the one-dimensional decomposition, secondary nodes are numbered consecutively after the last primary node. The primary node connectivity is increased by one neighbor, but

this poses no changes for the linear equation solver in FEHM. The logic is summarized as follows:

1. Read the GDPM input. This consists of identifying primary nodes that will be converted to GDPM nodes, the conceptualization of the of the GDPM model, the volume fraction of the primary node, and the refinement level for the secondary material,
2. Modify array allocations, add additional nodes, and modify nodal connectivity,
3. When solving the linear equations: (a) perform a one-dimensional decomposition for the secondary node variables, (b) solve for the primary node variables, and (c) back substitute for the secondary node variables.

Because the GDPM formulation is entirely geometric in nature, it is independent of subsurface physics. Besides the obvious application in representing subgrid-scale phenomena, GDPM can also represent far field conditions such as heat conduction from overburden or underburden layers by adding one-dimensional columns to the boundaries (Zyvoloski et al., 2007). GDPM is particularly useful when adding to or extending (via only input files) a pre-existing basin-scale FEHM model developed through tens of man-years of work in data collection, numerical model construction, and calibration.

Embedded Wellbore Model. Carbon sequestration, soil vapor extraction, and many petroleum industry applications require high-resolution wellbore models. As with the GDPM method, the unstructured connectivity in FEHM was used to embed a wellbore model (and surrounding casing, cement, and nearby rock) into a pre-existing numerical model with no modification other than adding few lines to input files. This yields a complete high-resolution, numerical radial model that is, like the GDPM model, independent of the physics package. The wellbore model simply replaces existing control volumes with the wellbore package. Figure 11 is an aerial view of a patch of primary nodes with rectangular control volumes defined by dotted lines. A wellbore model and its grid detail is also illustrated. Conceptually, operations are similar to those of the GDPM except that the added wellbore nodes have more connections than the GDPM model nodes thereby precluding the one-dimensional decomposition. The Embedded Wellbore Model (EWM) input requires well position and a model description including the outer radius of all included material surrounding the well and the desired layering in the radial and vertical directions. The operations are:

1. Read in position and EWM parameters,
2. Identify the primary nodes where the EWM will reside. This often includes multiple primary nodes in the direction of the well (usually vertical),
3. Remove volume from the primary nodes so that the model volume is conserved with the addition of the wellbore module,
4. Add connections (primary connectivity and wellbore nodes). It helps to start wellbore nodes numbering after the primary nodes,
5. Adjust the area factors for the primary nodes to account for the presence and location of the wellbore module with the primary gridblock.

The last operation listed above needs additional comment. With an EWM inserted into a control volume, the area factors from the primary node to its neighboring primary nodes

are adjusted to ensure the correct flow resistance from the wellbore model to the neighboring primary nodes. When the EWM is located off-center, as is shown in Figure 9, the area factor adjustments became asymmetric and are weighted to allow preferential communication to the nearest neighboring node outside the control volume in which the module resides. Pawar and Zyvoloski (2006) compared simulations with the wellbore module to high-resolution FD simulations and a control volume finite element simulation with high-resolution regriding of wellbore region. For a typical three-dimensional heat and mass transfer application, The FD method with telescoping grid resolution in the x and y directions required 2.5 times as many nodes and increased CPU time by about an order of magnitude. The regrided control-volume finite-element FEHM simulation was based on a grid with 12% more nodes and it required only 25% more CPU time. Both methods yielded equivalent results. Figure 12 compares the temperature fields at a depth close to the bottom of the well using the EWM module to one using the regrided control volume finite element for an injector-producer pair. All contour lines closely matched except $T = 100$, which is equal to the uniform initial background temperature. With the basic wellbore geometric formulation tested, future work on the EWM will include turbulent pipe-flow models for flow within the wellbore.

With few exceptions, all of the physics modules can use any of the sub grid scale features shown in Table 3.

APPLICATIONS

A sampling of FEHM applications with references are given in Table 2. Some of these papers are from a special Vadose Zone Issue (VZJ, August 2005, Volume 4, Issue 3) highlighting groundwater research at the Los Alamos National Laboratory. That issue contains additional papers (not mentioned in Table 2) with FEHM applications. The applications listed in Table 2, for the most part, are relatively large scale (hundreds of thousands of nodes or more). For those readers that are interested in basin scale groundwater flow, Keating et al (2003) and Rauskoff and Wolfsberg, eds. (2006) provide details of problem setups using FEHM and calibration results. In addition, Keating et al (2003) also describes the joint calibration of a high resolution site model and a basin scale model made possible by the CVFE method. While Tseng and Zyvoloski (2000) have already been mentioned in the context of efficient NR methods, the paper also provides a good introduction to the use of the CVFE method to model the heating of a nuclear waste repository due to radioactive decay. The paper features a high temperature application use of the multi-fluid (air and water) and multiphase (vapor, two-phase, and liquid) physics in FEHM. Kwicklis et. al (2006) uses the same physics package in a much lower temperature range to estimate near ground surface air and water vapor fluxes. Robinson et al. (2005) present a large scale simulation study of an unsaturated zone flow system that highlights the use of a tetrahedral based grid (shown in Figure 4) that follows the subsurface hydrostratigraphy. Chen et. al. (2007) present an application using FEHM to simulate the flow of NAPL and water in a heterogeneous permeability field. These

papers along with those already mentioned in the various sections presents above represent most of the features in FEHM.

COMPARISON WITH EXISTING SOFTWARE

In a previous section, the CVFE numerical method used in FEHM, was compared to the FE, FD, and IFD methods. In this section, FEHM will be compared to MODFLOW and TOUGH2. Comparisons of this sort are necessarily incomplete because these codes, like FEHM, are under continuous development. Many capabilities are being developed in current projects in beta versions of the software, will be available in subsequent versions. Nevertheless some general comparisons can be made.

FEHM and TOUGH2. Both TOUGH2 and FEHM are, as noted above, in continuous development. The codes have more similarities than differences. Both have many features related coupled heat and mass transfer as well as the ability to represent sub grid scale features. The reader is referred to Pruess (2004) or visit the TOUGH2 website (<http://www-esd.lbl.gov/TOUGH2/>) for an overview of TOUGH2 and current features. Both FEHM and TOUGH2 use a NR iteration. As described earlier, the IFD numerics of TOUGH2 and the CVFE numerics of FEHM are identical on grids that satisfy the Voronoi constraints and for diagonal permeability tensors. In this author's opinion, the main numerical differences between FEHM and TOUGH2 are:

1. FEHM uses analytic derivatives in the NR iteration. TOUGH2 uses numerical differences in its NR iteration.
2. FEHM has unique EOS functional forms described earlier. These facilitate the use of analytical derivatives.
3. FEHM has dual porosity methods and the GDPM method which utilize a fast 1D decomposition for the elimination of the secondary nodes. TOUGH2 does not "pre-solve" the matrix nodes of the dual porosity
4. FEHM has the Embedded Wellbore Module (EBM) described earlier.

The use of numerical derivatives in a NR iteration can also be an advantage for TOUGH2 in the development of new subsurface physics packages because of the extra coding and related debugging time necessary for the analytical derivatives.

TOUGH2 has an advantage in the area of parallel computing. Zhang et al., (2003) used a parallel computing version of TOUGH2 to simulate the unsaturated zone problem beneath Yucca Mountain with a high resolution (2 million nodes) grid. FEHM has, by comparison, crude parallel computing features. It does have module (*paractr*) that divides the problems into subdomains defined through user input. The domains communicate through ghost nodes and are individually renumbered. The FEHM formulation requires shared memory and convergence rates have been disappointing.

Important applications for both TOUGH2 and FEHM are CO₂ sequestration and nuclear waste isolation. Important for terrestrial CO₂ sequestration is a coupled mechanical model. Here the CVFE formulation in FEHM and the underlying FE grid provides the internal computations (briefly described in the section **NUMERICAL FORMULATION SUMMARY**) necessary to implicitly couple the flow, heat, and mechanical equilibrium equations. While TOUGH2 provides a very good solution to the flow equations, it lacks the additional geometric terms to define the mechanical equilibrium equations and sequential iteration with a mechanical stress code is required. Jing and Nguyen (2005) describe some approaches to sequentially coupling flow equations to the mechanical equilibrium equations suitable for FD and IFD codes.

FEHM and MODFLOW. FEHM and MODFLOW are both used in large scale applications for isothermal groundwater flow and transport. MODFLOW enjoys the world-wide recognition for its use in many applications and its acceptance in legal proceedings. Large scale here means 3D applications that have hundreds of thousands to over a million grid blocks. The MODFLOW flow solution is limited to single phase groundwater flow in confined and unconfined aquifer systems so the comparison with FEHM will be focused on features relevant to those applications. As noted earlier, the CVFE method is equivalent to the control volume FD method employed in MODFLOW. Here FEHM has advantages in numerical formulation, grid generation related to representing hydrostratigraphy and high resolution sub models. MODFLOW has advantages in speed, graphical user interfaces, and the existence of a large number of “packages” that facilitate the representation of complex boundary conditions. One of the drawbacks of MODFLOW when used for simulating unconfined aquifers is the solution of the highly nonlinear equations representing the flow of water through a partially filled gridblock with a Picard iteration technique. The formulation in FEHM effectively recasts the relationship between the saturation and hydraulic head in a partially filled gridblock in MODFLOW in a NR iteration with upwinding of interblock flow terms. This provides a much more stable and viable solution over a wide variety of input parameters. The unstructured grid used in FEHM allows for grid resolution to be varied according to problem requirements as shown in Figures 2 and 3. To obtain a similar resolution of the high flow units in Figure 2, with MODFLOW would require several times the number of FEHM gridblocks.

The flexibility of the FEHM and its CVFE formulation comes at a cost of additional computer memory and CPU-time requirements for some applications in comparison to FD methods. Zyvoloski and Vessilonov (2006) compared FEHM to MODFLOW on a simple steady-state confined aquifer problem with one variable (hydraulic head) on about 2 million orthogonal gridblocks. The large problem was chosen to minimize the fraction of computer time associated with input and output. FEHM reproduced the MODFLOW solution and took 1.2 times longer than MODFLOW on a windows-based PC.

FEHM and other unstructured grid codes, whether traditional finite-element or CVFE-based, use more memory than traditional finite difference codes. Additional memory requirements include:

1. Area factors or stiffness matrix. While FD codes require $\mathcal{N}_x + \mathcal{N}_y + \mathcal{N}_z$ coefficients to be saved, where \mathcal{N}_x , \mathcal{N}_y , and \mathcal{N}_z are respectively the number of gridblocks in the x, y, and z directions. FEHM requires saving $NEQ \times NEIGH / 2$ coefficients, where NEIGH is the average number of nodal connections per node with the division by 2 accounting for the fact that an area factor is used by two gridblocks.
2. The integer connectivity array requires storing $NEQ \times NEIGH + NEQ + 1$ integers. This array is not required for traditional finite difference code because the neighbors of any gridblock can be found in a FD code from the logical (structured) nature of the grid.
3. A connectivity array for the symbolic factorization that is required for preconditioner factorization levels greater than one, ILU(1). Behie and Vinsome (1982) demonstrated speedups using higher factorization levels with the preconditioner for thermal problems. FEHM requires an additional ILU connectivity array for ILU(2) and higher. For ILU(1), this array is not required because the connectivity of the preconditioner is identical to that for the Jacobian array described in step 2. Again, because of the structured grid, this additional array is not required for FD methods.
4. The computer memory required for the linear set of equations is often more for FEHM than the corresponding FD code because of additional connections for the CVFE method.
5. Because of the use of analytical derivatives in its Newton-Raphson iteration FEHM, allocates space for the derivatives of all parameters with respect to all active variables. This space is released prior to the linear solution phase of the NR iteration.

The additional storage described above is for simulations that generate symmetric linear systems such as those for confined aquifer simulations. For nonlinear flow problems, or linear flow problems with contaminant transport, parameter upwinding is often required. This puts additional constraints on the linear equation solver because the linear equations become unsymmetric and thereby require about twice the computer memory as symmetric problems for both the Jacobian and preconditioner matrix. Furthermore, required memory for the Krylov acceleration is always greater than those using conjugate gradient methods.

It should be noted that there has been collaboration between the USGS and the FEHM development team in the iterative coupling of MODFLOW and FEHM. This is especially important in those applications where existing models, created with many man-years of work must function together. As noted earlier, Dickenson et al. (2007) worked out flux-averaging schemes that allow flux continuity even when the grids do not match on model boundaries.

FEHM CODE STRUCTURE

FEHM is written in Fortran 77 and Fortran 90 with dynamically allocated memory and **use** modules for global communication. The basic code structure and flow diagram is shown in Figure 11. The block labeled **read input** indicates that the input files were “scanned” to determine computer memory requirements, allocate memory, and prepare needed physics packages. A complete description of all macros is found in the user’s manual (Zyvoloski et al., 1996). Of note in the **initialization** block is the FEHM feature that calculates and saves the area factors or that reads in factors calculated by the external grid generation program LaGriT (or calculated by a previous run of FEHM). The linear equation solver allows an arbitrary level of fill-in for the ILU-based preconditioner. The symbolic factorization process creates a connectivity array in CSR format for the preconditioner, similar to the nodal connectivity array, with additional connections where the fill-in occurs in factorization steps. This process is relatively time consuming and thus the symbolic factorization is created only once (and written to a file) for a given grid. These two operations greatly speed analyses comprising multiple runs of the same model with different parameters. For example, one of the current NTS confined aquifer models (shown in Fig. 2) has about 1.5 million nodes and it requires about 10 hours to generate the area factors and symbolic factorization. A steady-state run including time to read in the area factors and symbolic factorization is about 10 minutes.

The **time step loop** is used even for steady-state runs for both linear (e.g., single phase confined aquifer models) and nonlinear problems where the simulation is run over long times with increasing time step size until there is minimal difference between the inflows and outflows (the difference is specified in the input file). For linear models such as models representing confined aquifers, this might be a couple of time steps. For nonlinear models this could take thousands of time steps. In the **balance equations** block, all the material and energy balance equations are constructed and equation balances are monitored whether or not simplifying approximations, such as the RDOF method described earlier, are used in the solution of the coupled equations. The **linear equations** block solves the linear system for the NR variable updates. This is where RDOF and other techniques are used to simplify the preconditioner for the linear system. For GDPM applications, this is where one-dimensional decomposition occurs. This decomposition of the secondary nodes reduces the dimension of the linear equations to the number of primary nodes. In coupled physics problems (e.g. heat and mass transfer), one or more of the degrees of freedom are removed by neglecting terms in the linear system to allow pre-factoring of the degrees of freedom. The resulting linear system, often unsymmetric, is solved with preconditioned Krylov-space methods. After the solution of the linear system, the variables that were pre-eliminated during the GDPM decomposition or

through RDOF procedures are recovered by through back substitution. The **output** block provides output in SURFER, TECPLOT, AVS, and AVS EXPRESS formats.

The internal structure in FEHM uses controller modules to organize specific physics modules and other functions and the structure decreases development time for new physics modules. The controller for a particular physics module, for example the CO₂-Water-Heat module, reads input for the physics module, allocates memory, determines the phase state and independent variables, constructs the material and energy balance equations, updates the variables, and prints the controller-physics specific output. Newer modules (e.g., CO₂ and methane hydrate) employ keywords to further organize the input.

As mentioned previously, the input structure for FEHM is in the form of macro control statements followed by a group of input parameters for a specific function or property. These input macros are largely order independent. An important feature of FEHM, in contrast to traditional finite element computer codes, is the nodal definition of all parameters instead of the usual element (or quadrature) definition of parameters. This format allows exact duplication of finite difference solutions on orthogonal grids with the advantages of the CVFE method on irregular and sloping grids. An important part of FEHM's ability to test grids is the feature that allows definitions of arbitrary parts of numerical grid/domain without reference to node numbers (e.g., when assigning unique identifiers for properties such as permeability, porosity, layering, point sources, and boundary conditions). This is important in unstructured grids because the node numbering does not follow a predictable pattern as is the case with traditional structured finite difference codes such as MODFLOW. Zones can be defined geometrically by defining an arbitrary hexahedral polygon by its nodal coordinates. All nodes within the hexahedral polygon are assigned a unique number that can be used to assign permeabilities, porosities and other model parameters. LaGriT provides FEHM with the zone lists that identify the hydrostratigraphy and model boundaries for hydrostratigraphic surfaces provided from a solid earth model. The optimal grid resolution, balancing execution time and numerical error, can then be determined using only one set of input files that can test a number of grids with differing grid resolution.

RESEARCH PRIORITIES

Discretization methods. Permeability anisotropy can be important in upscaling fine grid data to larger grid blocks. Distorted and sloping grids are important in representing hydrostratigraphy and faults. Both anisotropy and grid distortion can be represented in a flux-continuous have algorithm developed by Lee et al. (1999). This has been implemented in FEHM although it is restricted to relatively isothermal single phase physics and transport. Improvements in memory usage and model restart efficiency are necessary to make it available for general use. Advanced finite-volume mimetic difference methods (Lipnikov et al., 2007) are also being actively investigated.

Advanced linear equation solvers. It is anticipated that future applications in CO₂ sequestration and energy programs will have mass and energy balances that are fully

coupled with the mechanical force balance equations. Initial testing has shown that Smoothed Aggregation Multigrid (Brezina et al., 2005) is very promising in solving systems of equations that include mechanical force balances. Reduced degree of freedom algorithms will continue to be important as the number of simulated fluids increases.

Parallelization and model coupling. Improvements in the parallelization of FEHM are necessary for studies that have many coupled processes at different scales. Multiple fluids and sufficient grid resolution will preclude the use of single processors on the basis of available computer memory alone. Parallelization of FEHM has much in common with implicit model coupling and both topics are being studied on several projects. The key will be the parallelization of the linear solver in the NR loop. The Smoothed Aggregation Multigrid method (Brezina et al., 2005) may come to bear because it is already parallelized and robustly solves systems of coupled equations.

CONCLUSIONS

The historical background and development of FEHM has been presented along with the CVFE numerical method and the solution algorithms for nonlinear multiphase problems. Major FEHM capabilities and features have been presented with development motivated by the following needs:

1. Numerical subsurface flow and transport models need to be created quickly and accurately from data provided by solid earth models such as EarthVision. This has been accomplished with the use of the LaGriT grid generation software and the ability of FEHM to represent distorted grids and areas of differing grid resolution.
2. Truncation errors and errors associated with mapping hydrostratigraphy need to be thoroughly evaluated. The ability to easily generate multiple grids of different resolution and to have input files that are largely independent of grid numbering allows these errors to be evaluated.
3. Flow regions requiring refined grid resolution need to be added with a minimum of effort to existing models. The LaGriT software and the CVFE numerics allow new grids with areas on high resolution to be generated with a minimum of effort.
4. Large, often nonlinear, numerical models must be stable and run efficiently in terms CPU time and computer memory usage. This is accomplished with the CVFE formulation in FEHM.
5. Multiple model runs, often numbering in the thousands, required by calibration and uncertainty analyses require special processing of area factors, symbolic factorization, and parameter input. The interface with the PEST software helps accomplish this task.
6. Subgrid scale and other multi-porosity processes need to be added easily to pre-existing input data. Subgrid scale processes (for example contaminant diffusion from impermeable layers) are often more important in transport calculations, which are typically run after a flow model has been developed and calibrated. The GDPM capability addresses this need.
7. Accurate simulations of near wellbore flow are critical to the simulation of geologic CO₂ sequestration and unconventional energy extraction from shale and

oil sands. The EWM allows detailed wellbore simulations to be added to existing models.

FEHM is a result of decades of effort by many researchers at many institutions.

SOFTWARE AVAILABILITY

The version of FEHM with the capabilities listed above is available at no cost at the website: <http://fehm.lanl.gov/>. The user is required to sign a single-user or single-institution license to help maintain version control. The code comes with an installation package that includes many example input sets that not only check the installation but provide useful examples (Dash, 2002).

ACKNOWLEDGEMENTS

Development of FEHM was funded by a variety of sources including geothermal (Hot Dry Rock), CO₂ sequestration, and radioactive waste isolation programs. The bulk of funding has come from the Yucca Mountain Project. Researchers at the Advanced Institute for Science and Technology (AIST) in Tsukuba, Japan also improved the coding related to mechanical fracture behavior and the methane hydrate module. Scott James carefully read this paper and his comments greatly improved it. Finally, the author would like to thank several anonymous reviewers who comments greatly improved the final manuscript.

Software References:

EARTHVISION 2007, <http://www.dgi.com/earthvision>.

EASYMESH, 2007, <http://www-dinma.univ.trieste.it/nirftc/research/easymesh/>.

GoCad 2007, <http://www.gocad.org>.

LaGriT, 2007, Los Alamos Grid Toolbox (LA-CC-99-0017, <http://lagrit.lanl.gov>).

MODFLOW-LGR, 2005, Local grid refinement package,
http://water.usgs.gov/nrp/gwsoftware/modflow2005_lgr/mflgr.html

PEST, 2007, <http://www.sspa.com/pest/>, developed by John Doherty of Watermark Numerical Computing, Australia.

STRATAMODEL 2007, <http://www.lgc.com> (note Stratamodel is older software and the level of support by Landmark Graphics is unclear).

REFERENCES

Behie A. and P.K.W. Vinsome, 1982, Block iterative methods for fully implicit reservoir simulation, *SPEJ*, 658–668.

Blackett, S.A., 1996, *Rational Polynomials*, Internal Uniservices Ltd. Publication, University of Auckland, New Zealand.

Bower, K.M., Gable, C.W., and G.A. Zyvoloski, 2005, Grid resolution study of ground water flow and transport, *Ground Water*, **43**(1), 122–132.

Brezina M., R. Falgout, S. MacLachlan, T. Manteuffel, S. McCormick, and J. Ruge, 2005, Adaptive smoothed aggregation (ASA) multigrid, *SIAM Review SIGEST*, **47**, 317–346.

Bower, K. M., and G. Zyvoloski, 1997, “A Numerical Model for Thermo-Hydro-mechanical Coupling in Fractured Rock,” *Int. J. Rock Mech. Min. Sci.* Vol. 34, No. 8., pp. 1201-1211.

Bullivant, D. and G.A. Zyvoloski, 1990, *An efficient scheme for the solution of linear system arising from coupled differential equations*, Los Alamos Report LA-UR-90-3187.

- Chen M., A. Keller, D. Zhan, Z. Lu, and G.A. Zyvoloski ,2007, A stochastic analysis of transient two-phase flow in heterogeneous porous media, accepted for publication in *Water Resour. Res.*.
- Chen, M. and G.A. Zyvoloski, 2006, Model coupling with control volume finite elements, *MODFLOW and MORE 2006 Conference: Managing Ground-Water Systems*, Golden, CO.
- Dalen, V., 1979, Simplified finite-element models for reservoir flow problems, *Soc. Pet. Eng. J.*, **19**, 333–343.
- Dash, Z. V., 2002, *Attachment 1, Validation Test Plan (VTP) Results, FEHM V2.20 Validation Test Plan 10086-VTP-2.20-00*, available on the web: <http://fehm.lanl.gov/>
- Dickinson J.E., S.C. James, S.W. Mehl, M.C. Hill, S.A. Leake, G.A. Zyvoloski, and A.-A. Eddebbarh, 2007, A new ghost-node method for linking different models and initial investigations of heterogeneity and nonmatching grids, *Adv. Water Resour.*, Volume 30, Issue 8, August 2007, Pages 1722-1736.
- Doherty, J., 2006, Fast lookup of CO₂ properties, Watermark Computing Inc. (Australia), Report June 2006.
- Forsyth, P. A., 1990, A control-volume finite-element method for local mesh refinement, *SPERE* (Nov. 1990), pp 561-566.
- Faust, C.R. and J.W. Mercer, 1976, A comparison of finite difference and finite element techniques applied to geothermal reservoir simulation, Paper SPE 5742, Presented at the *SPE-AIME Fourth Symposium on Numerical Simulation of Reservoir Performance*, Los Angeles, California.
- Fung, L.S.-K., Heibert, A.D., and L.X. Nghiem, 1992, Reservoir simulation with a control volume finite-element method, *SPERE* (August 1992), pp 348-357.
- Gable C.W., H. Trease, and T. Cherry, 1996, Geological applications of automatic grid generation tools for finite elements applied to porous flow modeling, in *Numerical Grid Generation in Computational Fluid Dynamics and Related Fields*, edited by B. K. Soni, J. F. Thompson, H. Hausser and P. R. Eiseman, Engineering Research Center, Mississippi State Univ. Press.
- Gangi, A.F., 1978. Variation of whole and fractured porous rock permeability with confining pressure. *Int. J. Rock Mech. Min. Sci. & Geomech. Abstr.* 15, 249-257.
- Gerke, H.H. and M.T. van Genuchten, 1993, Evaluation of a first-order water transfer term for variably saturated dual-porosity flow models, *Water Resour. Res.*, **29**(4), 1225–1238.

- George, A. and J.W.-H. Liu., 1981, *Computer solution of large sparse positive definite systems*, Computational Mathematics, Prentice-Hall.
- Harbaugh, A.W., E.R. Banta, M.C. Hill, and M.G. McDonald, 2000, *MODFLOW 2000, The U.S. Geological modular ground-water model—User guide to modularization concepts and the ground-water flow process*, U.S. Geological Survey Open-File Report 90-392.
- Hammond, G.E., 1999 Verification of the Kinetic Precipitation-Dissolution Reaction in the Finite Element Heat and Mass Transfer Code (FEHM), M.S. Thesis, University of Illinois, Champaign-Urbana, Illinois.
- Harr, L., J. Gallagher, and G.S. Kell, 1984, *NBS/NRC Steam Tables, Thermodynamics, and Transport Properties and Computer Programs for Vapor and Liquid States of Water*, Hemisphere Press.
- Haukwa, C.B., Y.W. Wu, and G.S. Bodvarsson, 2003, Modeling thermal-hydrological response of the unsaturated zone at Yucca Mountain Nevada to the thermal load at a potential repository, *J. Cont. Hydrol.*, **62**, 529–552.
- Jenny, P., Wolfsteiner, C., Lee, S.H., and L. J. Durlofsky, Modeling flow in geometrically complex reservoirs using hexahedral multi-block grids, *SPE Reservoir Simulation Symposium*, Houston, Texas, 11-14 February 2001.
- Jing, L., and T.S. Nguyen (ed.), 2005, DECOVALEX III/BENCHPAR Projects, *Implications of Thermal-Hydro-Mechanical Coupling on the Near-Field safety of a Nuclear Waste Repository*, SKI Report 2005:24, 92 pages.
- Kelkar, S. and G.A. Zyvoloski, 1991, An efficient three dimensional fully coupled hydro-thermal-mechanical simulator: FEHMS, *11th SPE Symposium on Reservoir Simulation*, Anaheim, California, February 1991.
- Keating, E.H., V.V. Vesselinov, E. Kwicklis, and Z. Lu, 2003, Coupling large- and local-scale inverse models of the Española Basin, *Ground Water* **41**(2), 200–211.
- Kwicklis, E.M., A.V. Wolfsberg, P.H. Stauffer, M.A. Walvroord, and M.J. Sully, 2006, multiphase multicomponent parameter estimation for liquid and vapor fluxes in deep arid systems using hydrologic data and natural environmental traces, *Vadose Zone J.*, **5**:934-950.
- Lee, S. H., H. Tchelepi, and L.F. DeChant, 1999, Implementation of a flux-continuous finite difference method for stratigraphic, hexahedral grids, SPE paper 51901, the *Proceedings of the SPE Symposium on Reservoir Simulation*, 231–241.

- Lipnikov K., M. Shashkov, D. Svyatskiy, Y. Vassilevski, 2007, Monotone finite volume schemes for diffusion equations on unstructured triangular and shape-regular polygonal meshes, Los Alamos Report, LA-UR-07-2886.
- Manteuffel, T.A., 1980, An incomplete factorization technique for positive definite linear system, *Mathematics Comp.*, 473–497.
- Mehl, S.W. and M.C. Hill, 2002, Development and evaluation of a local grid refinement method for block-centered finite-difference ground-water models using shared nodes, *Adv. Water Resour.*, 25, 497–511.
- Mercer, J.W. and C.R. Faust, 1975, Simulation of water- and vapor-dominated hydrothermal reservoirs, Paper SPE 5520, Proceedings of the 50th Annual Fall Meeting of the Soc. Pet. Eng. of AIME, Dallas, Texas.
- Mercer J. W., and G.F. Pinder, 1973, Galerkin Finite Element Simulation of a Geothermal Reservoir”, *Geothermics*, Vol 2, pp81-89.
- Moore, C. and J. Doherty, 2005, The role of the calibration process in reducing model predictive error, *Water Resour. Res.*, 41 W05020, doi:10.1029/2004WR003501.
- Neuman, S.P. and P.A. Witherspoon, 1970, Finite element method of analyzing steady seepage with a free surface, *Water Resources Res.* 6(3), 889–897.
- Neuman, S.P., 1973, Saturated-unsaturated seepage by finite elements, *J. Hydraul. Division, ASCE*, 99(HY12), 2223–2249.
- Nitao, J.J., 1998, *Reference Manual for the NUFT Flow and Transport Code, Version 2.0*, Lawrence Livermore National Laboratory, Livermore, CA (UCRL-MA-130651)
- Pollock D.W., 1989, Documentation of computer programs to compute and display pathlines using results from the U.S. Geological Survey modular three-dimensional finite-difference ground-water model, USGS Open-File Report 89-381, 188 pp.
- Pawar, R.J. and G.A. Zyvoloski, 2006, A novel method to couple wellbore flow to reservoir flow, *XVI International Conference on Computational Methods in Water Resources*, Copenhagen, Denmark.
- Pawar, R.J., 2007, Numerical simulations of large-scale CO₂ injection incorporating effect of potential wellbore leakage”, Proceedings of the 2007 DOE Conference on Carbon Capture & Storage, May 7-10, 2007, Pittsburgh, PA.
- Pruess, K., 1991, *TOUGH2 - A general-purpose numerical simulator for multiphase fluid and heat flow*, Lawrence Berkeley Laboratory Report LBL-29400.

- Pruess, K. and T.N. Narasimhan, 1985, A practical method for modeling fluid and heat flow in fractured porous media, *Soc. Pet. Eng. J.*, **25**, 14–26.
- Richards, L.A. 1931. Capillary conduction of liquids through porous mediums, *Physics*, 1318–333.
- Robinson, B.A., G. Cole, J.W. Carey, M. Witkowski, C.W. Gable, and R. Gray, 2005, A vadose zone flow and transport model for Los Alamos Canyon, Los Alamos, New Mexico, *Vadose Zone J.* **4**(3), 729–743.
- Robinson, B.A., H.S. Viswanathan, and A.J. Valocchi, 2000, Efficient numerical techniques for modeling multicomponent ground-water transport based upon simultaneous solution of strongly coupled subsets of chemical components, *Adv. Water Resour.*, **23**, 307–324.
- Ruskauff, G.J., and A.V. Wolfsberg (leads), et. al., 2006, Groundwater Flow Model of Corrective Action Units 101 and 102: Central and Western Pahute Mesa, Nevada Test Site, Nye County, Nevada, Stoller Navarro Joint Venture Technical Report, S-N/99205076, Las Vegas, NV.
- Smith, E.H. and M.S. Seth, 1999, Efficient solution for matrix-fracture flow with multiple interacting continua, *Int. J. Num. Anal. Meth. Geomech.* **23**, 427–438.
- Tenma, N., Y. Yamaguchi, and G.A. Zyvoloski, 2007, Estimation of characteristics of the multi-reservoir at the Hijiori Hot Dry Rock test site during a long-term circulation test, accepted for publication, *Geothermics*.
- Thomas, L.K., 1978, Three dimensional geothermal energy simulation, *Soc. Pet. Eng. J.*, 151–161.
- Tseng, P. H. and G.A. Zyvoloski, 2000, A reduced degree of freedom method for non-isothermal multi-phase flow in porous medium, *Adv. Water Res.*, **23**, 731–745.
- Van der Vorst, H.A., 1992, Bi-CGSTAB: A fast and smoothly converging variant of Bi-CG for the solution of nonsymmetric linear systems, *SIAM J. Sci. Statist. Comput.*, **13**, 631–644.
- Viswanathan, H.S., 1996, Modification of the finite element heat and mass transfer code (FEHMN) to model multicomponent reactive transport. M.S. Thesis, University of Illinois, Champaign-Urbana, Illinois, September 1995. Los Alamos National Laboratory Report LA-13167T.
- Viswanathan, H.S., B.A. Robinson, A.J. Valocchi, and I.R. Triay, 1998, A reactive transport model of neptunium migration from the potential repository at Yucca Mountain, *J. Hydrol.*, **209**, 251–280.

- Voronoi, G.F., 1908, Nouvelles applications des param`etres continus `a la th`eorie des formes quadratiques. Deuxi`eme memoire: Recherches sur les parall`ello`edres primitifs. *J. reine angew. Math.* 134, 198–287.
- Vrugt, J.A., and B.A. Robinson, 2007, Improved evolutionary optimization from genetically adaptive multimethod search, *PNAS*, doi:10.1073/pnas.0610471104.
- Vrugt, J.A., 2007, Inverse modeling of subsurface flow and transport properties using recent advances in global optimization, parallel computing and sequential data assimilation”, *Vadose Zone Journal* (this issue).
- Warren, J.E. and P.J. Root, 1963, The behavior of naturally fractured reservoirs, *Soc. Pet. Eng. J.*, **3**, 245–255.
- Watts, J.W., 1986, A compositional formulation of the pressure and saturation equations, *Soc. Pet. Eng. Res. Engr.*, 243–252.
- Zhang, K., Y. S. Wu and G. S. Bodvarsson, 2003, “Massively Parallel Computing Simulation of Fluid Flow in the Unsaturated Zone of Yucca Mountain, Nevada,” LBNL-48883, *Journal of Contaminant Hydrology*, pp.381-399.
- Zyvoloski, G.A., 1975, *Finite element solution of the two-dimensional unsaturated flow equation*, Ph.D. Thesis, Mechanical and Environmental Engineering Department, University of California, Santa Barbara.
- Zyvoloski, G. and M.J. O’Sullivan, 1980, Simulation of a gas-dominated two-phase geothermal reservoir, *Soc. Pet. Eng. J.*, 52-58.
- Zyvoloski, G., J.C. Bruch, and J.M. Sloss, 1976, Solution of equation for two-dimensional infiltration problems, *Soil Science*, **122**, 65–70.
- Zyvoloski, G.A., M.J. O’Sullivan, and D.E. Krol, 1979, Finite difference techniques for modelling geothermal reservoirs, *Int. J. Anal. and Num. Meth. Geomech.*, **3**, 355–366.
- Zyvoloski, G., 1983, Finite element models for geothermal reservoir simulation, *Int. J. Anal. and Num. Meth. in Geomech.*, **7**, 75–86.
- Zyvoloski, G., 1986, Incomplete factorization for finite element methods, *Int. J. Num. Meth. Eng.*, **23**, 1101–1109.
- Zyvoloski, G., 1989, Efficient matrix procedures for the simulation of coupled processes, *1989 Eastern Multiconference*, Tampa, Florida, Los Alamos National Laboratory Document LA-UR-88-4274.

Zyvoloski, G.A., Z.V. Dash, and S. Kelkar, 1992, *FEHMN 1.0: Finite Element Heat and Mass Transfer Code*, LA-12062-MS, Rev. 1.

Zyvoloski, G.A., B.A. Robinson, Z.V. Dash, and L.L. Trease, 1996, *Users manual for the FEHMN application*, Los Alamos Report LA-UR-94-3788, Rev. 1.

Zyvoloski, G.A., B.A. Robinson, Z.V. Dash, and L.L. Trease, 1997, *Models and methods summary for the FEHMN application*, Los Alamos Report LA-UR-94-3787, Rev. 1.

Zyvoloski, G.A., and E. Keating, 2005, A numerical approach to efficiently simulate wetting and rewetting in a transient unconfined simulation, GSA annual meeting, October 2005, Salt Lake City, Utah.

Zyvoloski George A., and V. V. Vesselinov, 2006, "An Investigation of Numerical Grid Effects in Parameter Estimation", *Ground Water* 44 (6), 814–825. doi:10.1111/j.1745-6584.2006.00203.x

Zyvoloski, G.A., B.A. Robinson, and H.S. Viswanathan, 2007, Generalized double porosity: A method for representing spatially variable sub-grid scale processes, Los Alamos Report, LAUR-07-3486, in review, *Advances in Water Resources*.

Zyvoloski, G., 2007, FEHM: A control volume finite element code for simulating subsurface multi-phase multi-fluid heat and mass transfer. Los Alamos National Laboratory Document LAUR-07-3359.

Table 1. Summary and Time line for FEHM developments

Key Development	Reference
Representation of nonlinear terms with shape functions. Assembly of finite element equations by node rather than elements. Separation of geometric and fluid parts of Finite element stiffness matrix.	Zyvoloski (1975) Zyvoloski et. al. (1976)
Formulation and solution of two-phase fully coupled heat and mass transfer equations in primitive form using Newton-Raphson iteration. Two independent variables. Block-centered finite difference discretization.	Zyvoloski et al (1979)
Extension of techniques to include non-condensable gas (CO ₂). Three independent variables.	Zyvoloski and O'Sullivan (1980)
Combination of non-linear solution techniques	Zyvoloski (1983)

with finite element method. In the finite element stiffness matrix the nonlinear terms were separated from the geometric parts. Equivalence of finite difference and finite element methods obtained through choice of integration points in stiffness matrix. Tradition unwinding techniques used with finite element methods.	
Development of variable level incomplete factorization pre-conditioner for unstructured grid. Used with Krylov space acceleration method to solve the linear equations associated with the Newton Raphson method.	Zyvoloski (1986)

Table 2. Physics module and features available in FEHM

Subsurface Process or Feature	Independent Variable(s)	Selected Reference
Confined and unconfined aquifers, unsaturated-saturated flow including Richards' equation	hydraulic head	Keating et al. (2003) Zyvoloski (2005)
Non isothermal water and water vapor	pressure, temperature or saturation (variable switching)	Temma et al (2007)
Isothermal air-water multiphase flow	pressure, saturation	Robinson et al. (2005)
Non isothermal air-water-water vapor-heat flow	pressure, temperature, partial pressure of air or saturation	Kwicklis et al. (2006), Tseng and Zyvoloski (2000)
Coupled thermal hydrological flow mechanical equilibrium	pressure, temperature, displacements in the x, y, and z directions	Bower and Zyvoloski (1997)

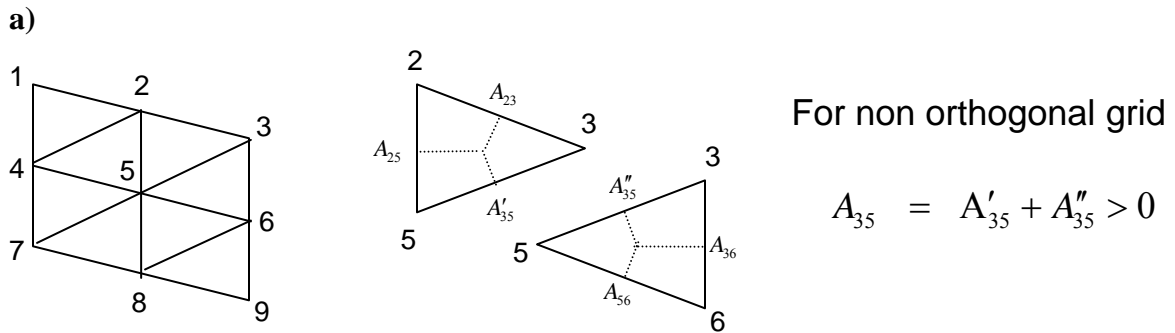
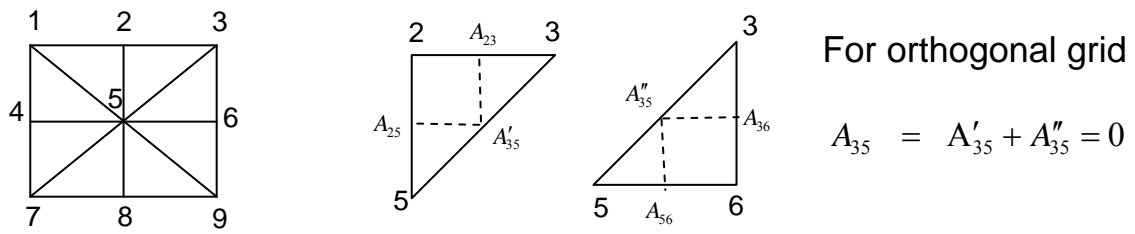
Non isothermal-CO ₂ -water	pressure, partial pressure of CO ₂ or mass fraction of CO ₂ , saturation of CO ₂ , temperature	Pawar et al. (2007)
Non isothermal Methane hydrate dissociation- water-methane	Kinetic model: Pressure, temperature, water saturation, hydrate fraction. Equilibrium model: Combinations of 3 variables in kinetic model.	Pawar et al (2004)
Isothermal NAPL (oil)-Water	Pressure, saturation	Chen et al. (2007)
Transport and reactive transport	Different combinations, see reference.	Robinson et al. (2000)

Note; Pressure means total system pressure

Table 3. Subgrid scale features available in FEHM

Subgrid scale feature		Selected Reference
Dual porosity		Zyvoloski et al (1991)
Generalized dual porosity		Zyvoloski et al. (2007)
Dual permeability		Tseng and Zyvoloski (2000)
Embedded wellbore model		Pawar and Zyvoloski (2006)

FIGURES



b)

Figure1. Definition of Control Volume Areas in the CVFE method. a) orthogonal grid b) non orthogonal grid.

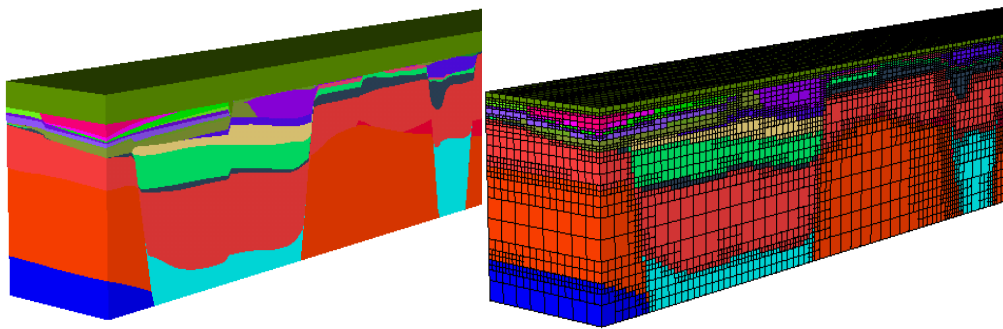


Figure 2. Grid generation with LaGriT showing a hexahedral-based grid with octree refinement.

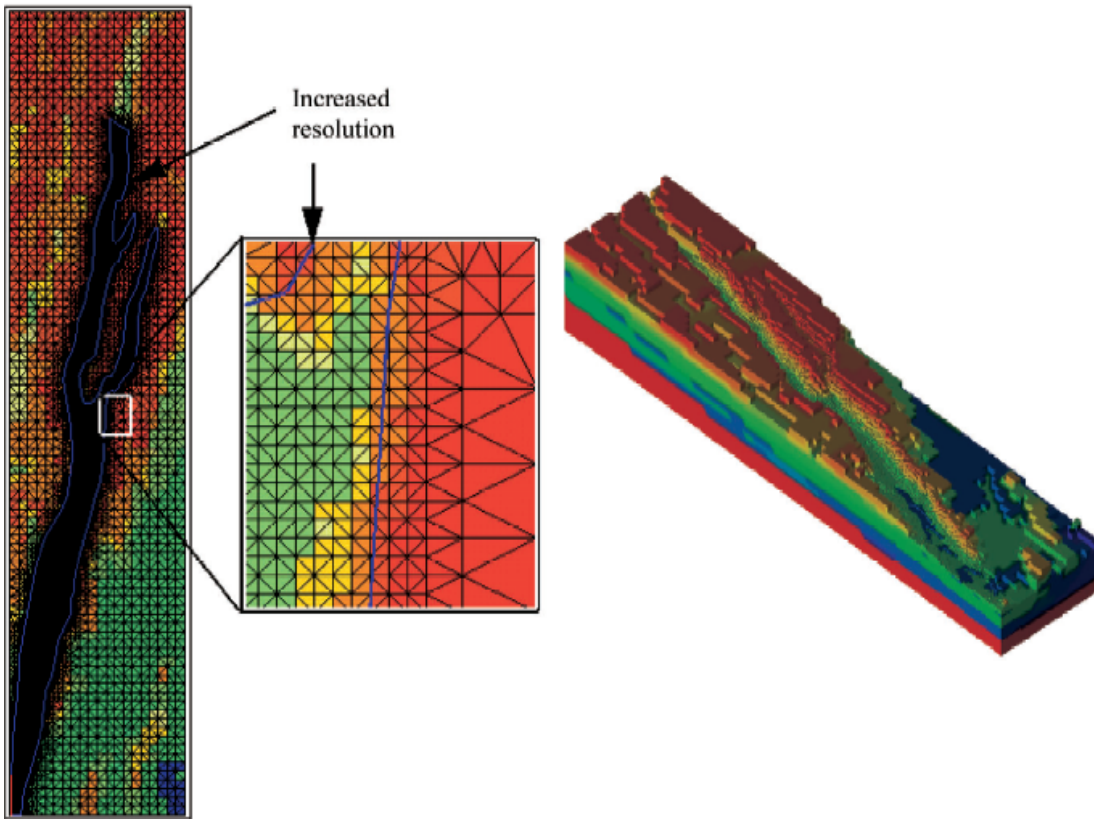


Figure 3. Tetrahedral-based grid of a unsaturated zone flow system

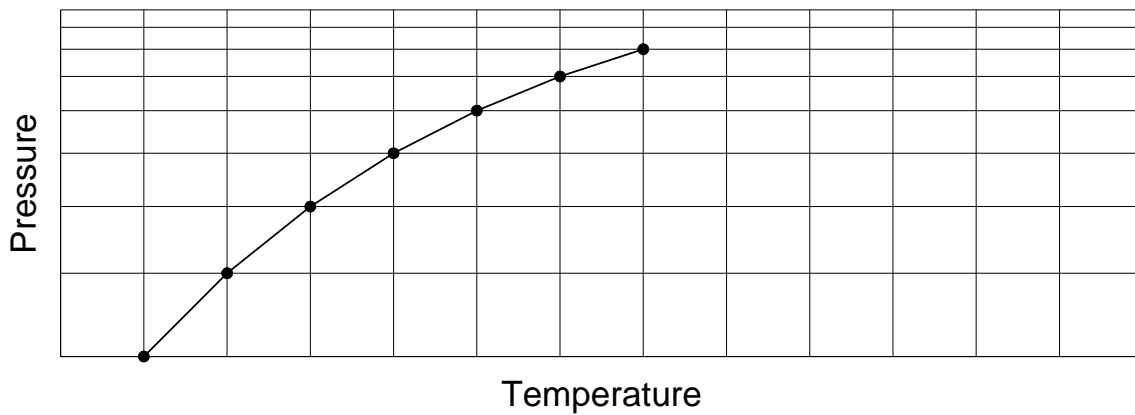


Figure 4. Tabular interpolation on a variably spaced grid with a phase transition line-grid with variable pressure spacing and uniform temperature spacing.

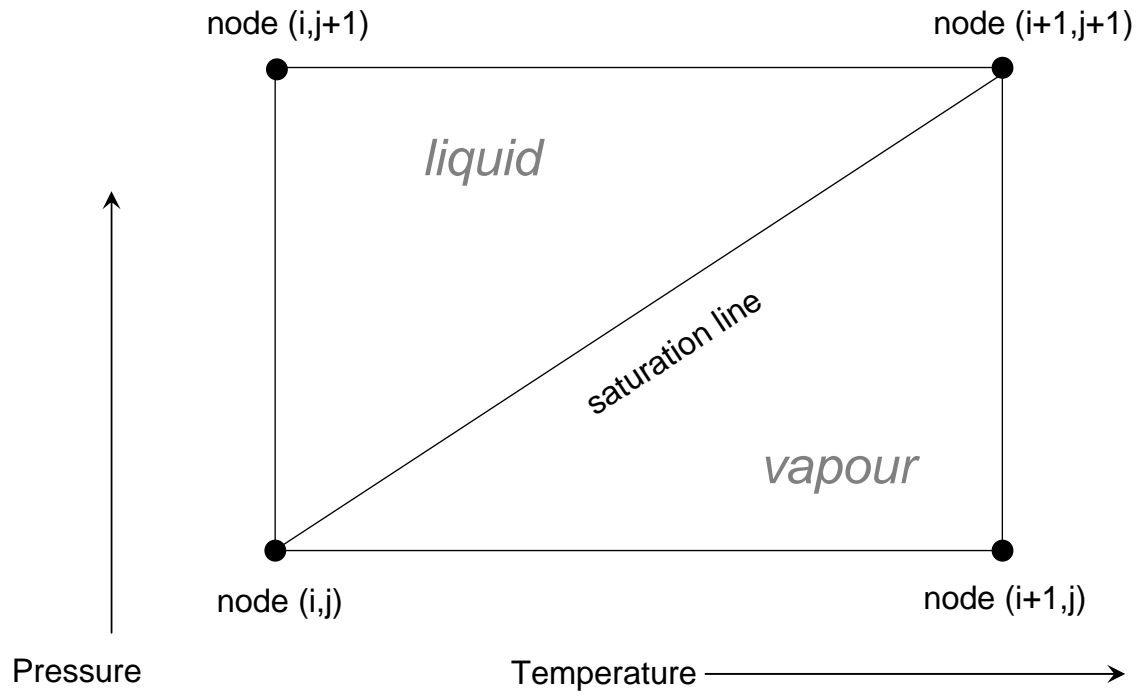


Figure 5. Tabular interpolation on a variably spaced grid with a phase transition line. - detail of a block with phase line.

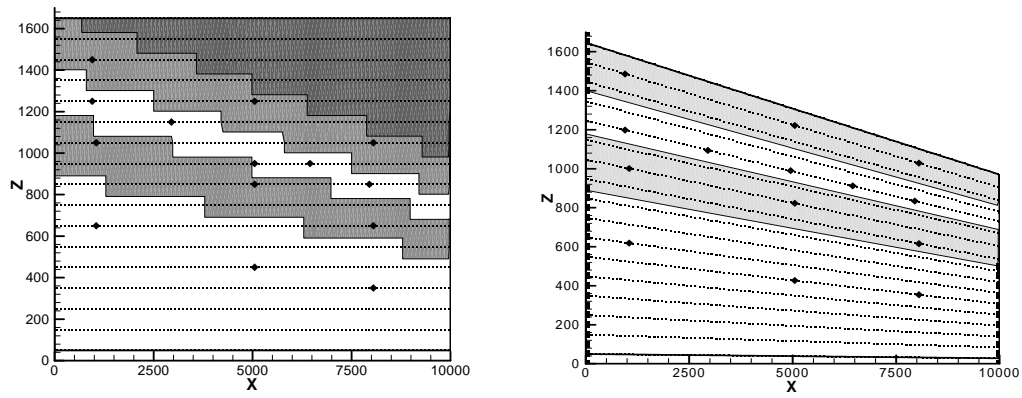


Figure 6. Sloping stratigraphy represented with a coarse finite difference grid and a grid with sloping coordinates.

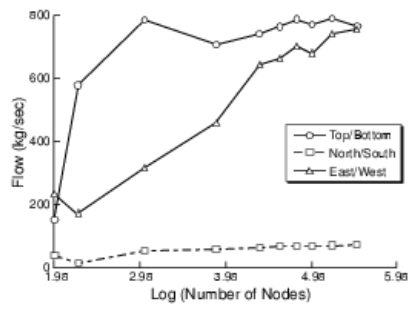
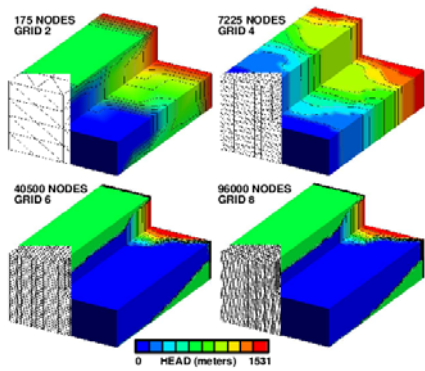
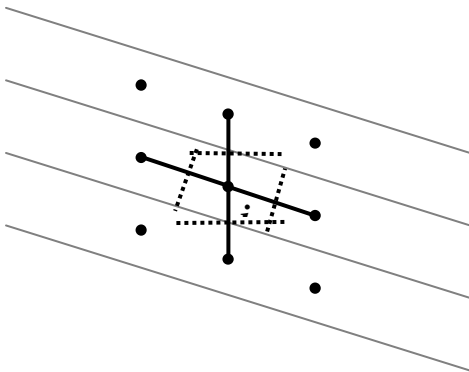
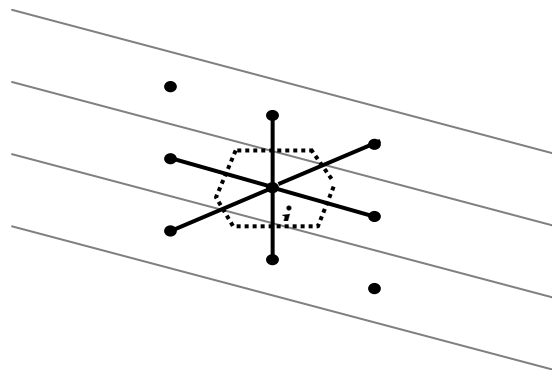


Figure 7. Grid testing with multiple grids

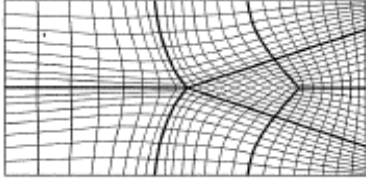


a. FD



b. CVFE

Figure 8. Control volumes on sloping grids. a. standard FD 5 point connectivity
b. CVFE connectivity



a)

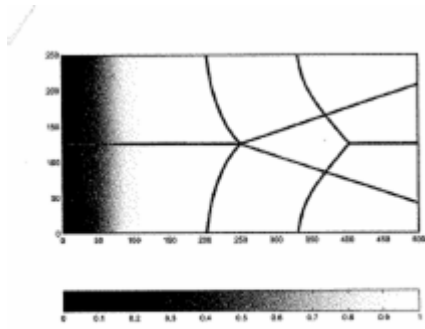


Figure 5: Displacement front at $t = 100$ d, 7-point stencil.

b)

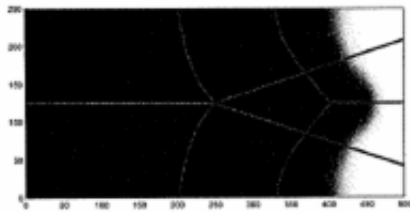


Figure 6: Displacement front at $t = 1000$ d, 7-point stencil.

c)

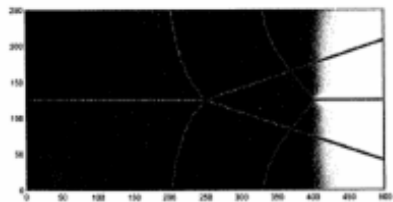
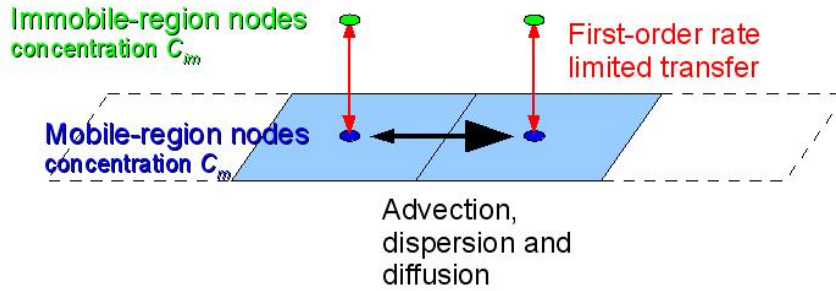


Figure 7: Displacement front at $t = 1000$ d, 27-point stencil.

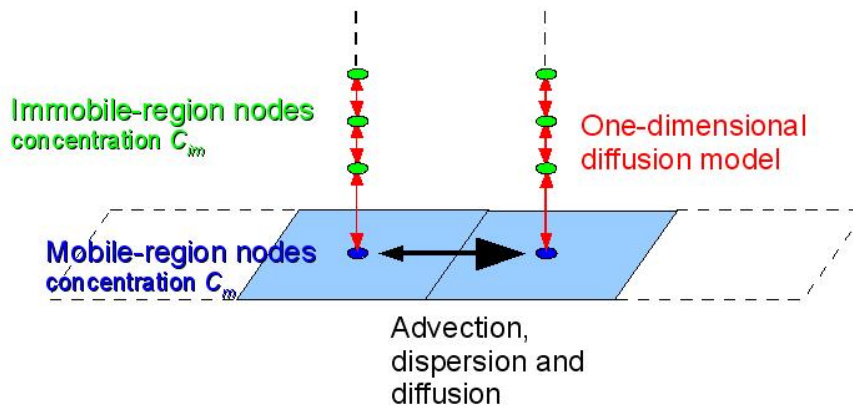
d)

Figure 9. Consequences of using a CFD stencil (7 point stencil in 3D) with a non orthogonal grid with transport. a) vertical crosssection of 3D grid, b) the flow away from

the non-orthogonal portion of the grid, c) the transport front produced with the CFD point stencil and d) the correct front produced with a 27 point stencil.



a)



b)

Figure 10. Double porosity models a) Traditional double porosity method with one immobile node. b) Generalized double porosity with multiple immobile nodes.

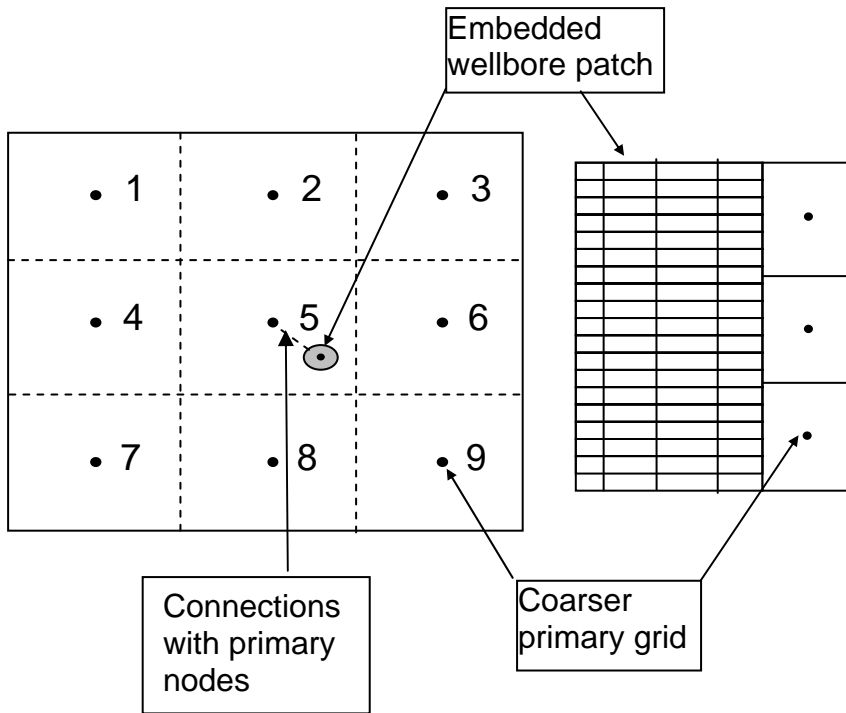


Figure 11 Conceptual description of the Embedded Wellbore Model (EWM).

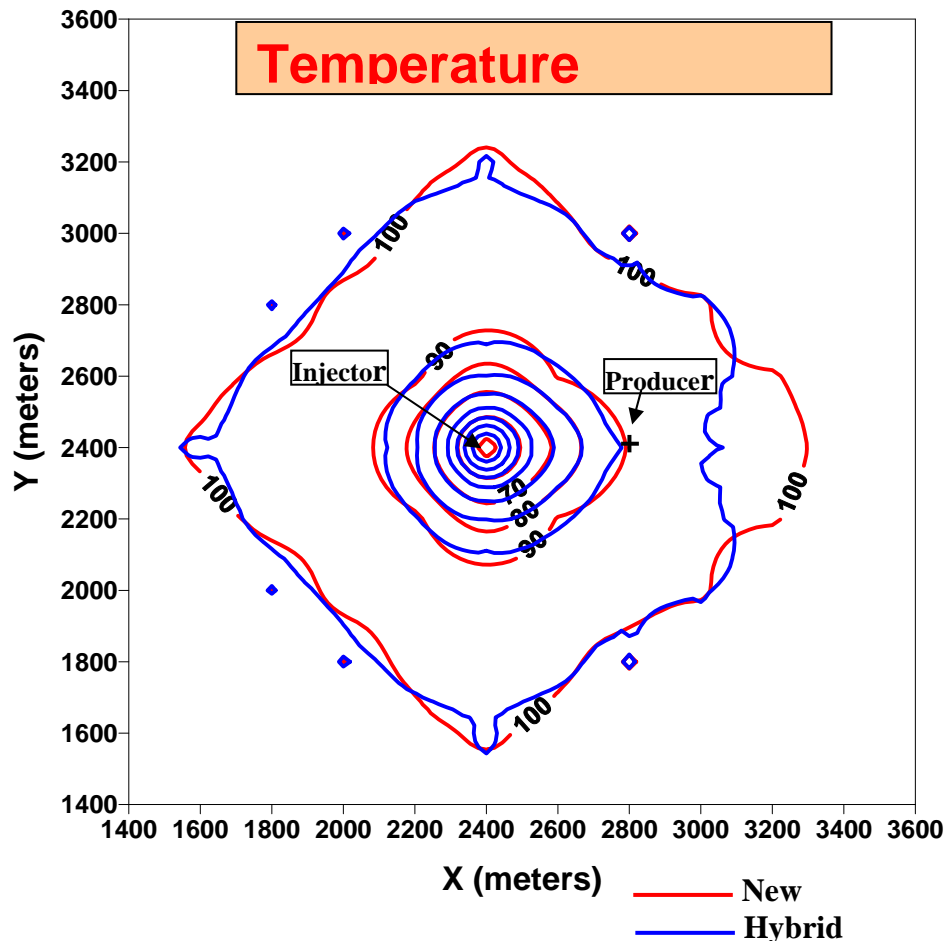


Figure 12. Comparison of EWM simulation with a re-gridded CVFE simulation Note the contour $T=100$ is also the initial uniform temperature and thus susceptible to noisy contours.

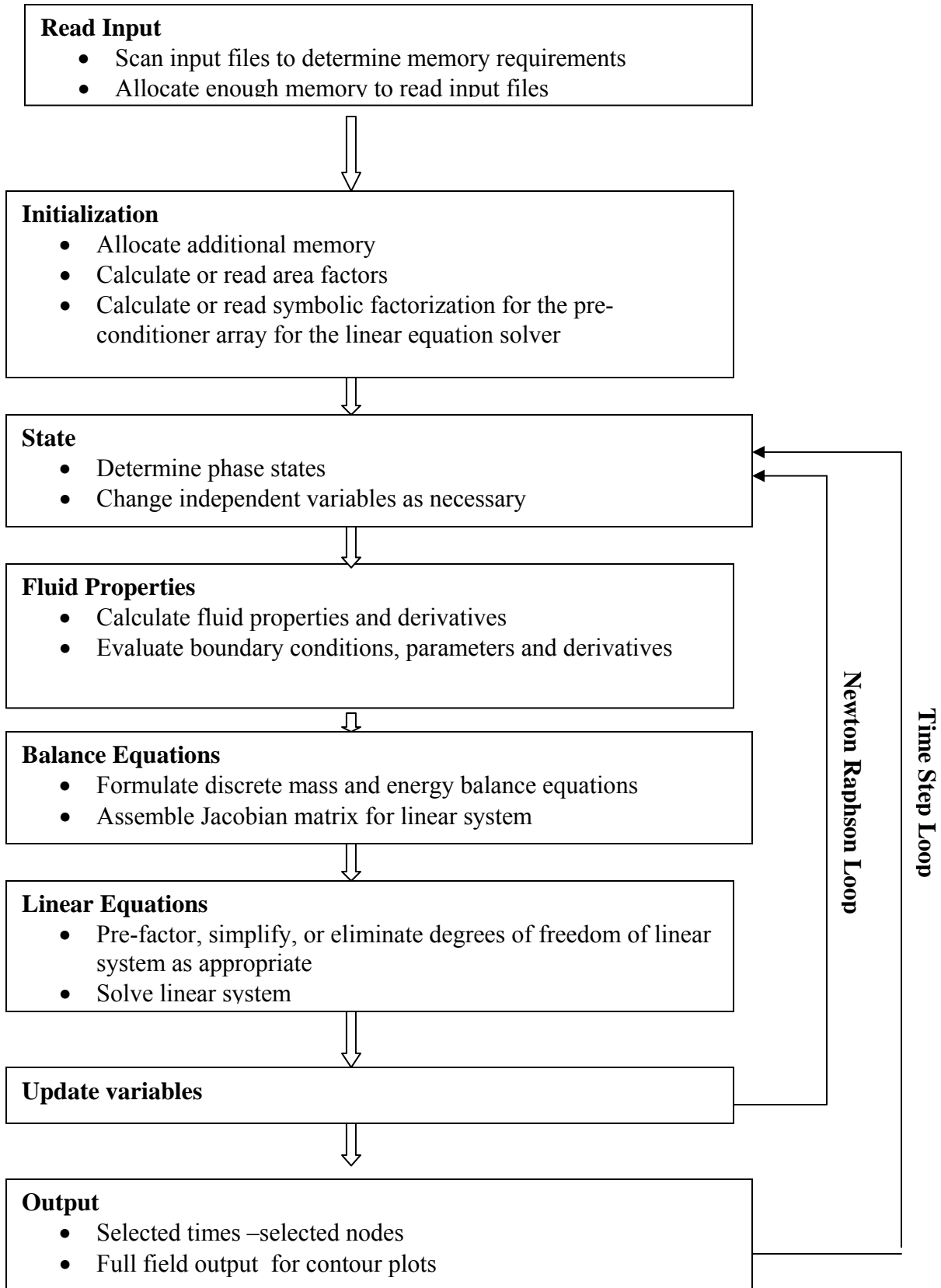


Figure 13. Flow diagram for FEHM

